Journal Pre-proof

Canagliflozin combined with aerobic exercise protects against chronic heart failure in rats

Helin Sun, Bingyu Du, Hui Fu, Zhaodi Yue, Xueyin Wang, Shaohong Yu, Zhongwen Zhang

PII: S2589-0042(24)00235-9

DOI: https://doi.org/10.1016/j.isci.2024.109014

Reference: ISCI 109014

To appear in: *ISCIENCE*

Received Date: 5 July 2023

Revised Date: 1 December 2023

Accepted Date: 22 January 2024

Please cite this article as: Sun, H., Du, B., Fu, H., Yue, Z., Wang, X., Yu, S., Zhang, Z., Canagliflozin combined with aerobic exercise protects against chronic heart failure in rats, *ISCIENCE* (2024), doi: https://doi.org/10.1016/j.isci.2024.109014.

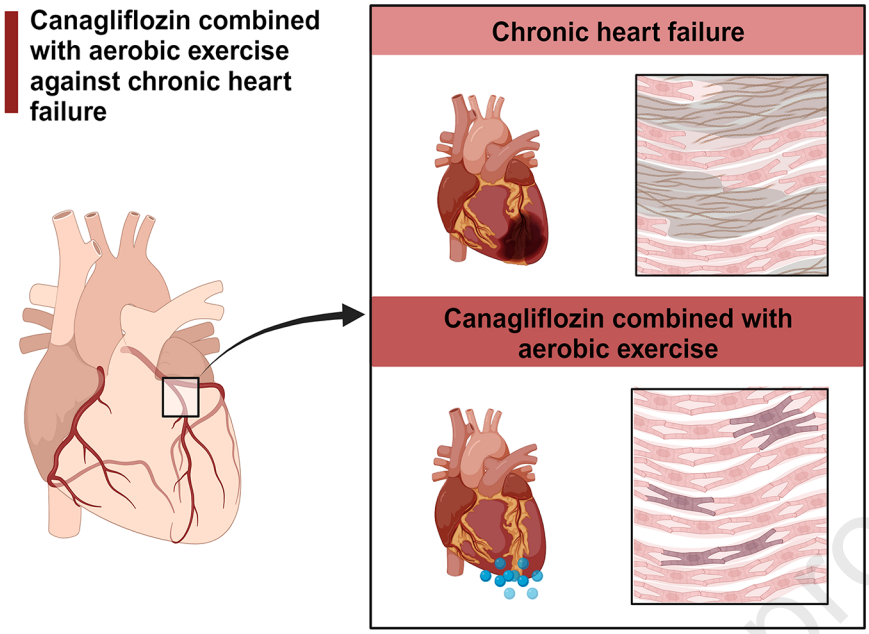

Canagliflozin combined with aerobic exercise protects against chronic heart failure in rats

Helin Sun[1†], Bingyu Du[1†], Hui Fu[5], Zhaodi Yue[3,4], Xueyin Wang[2], Shaohong Yu[3,4*], Zhongwen Zhang[2*]

[1] Department of Endocrinology and Metabology, Shenzhen Research Institute of Shandong University, shenzhen, China, Shandong Provincial Key Laboratory for Rheumatic Disease and Translational Medicine, The First Affiliated Hospital of Shandong First Medical University & Shandong Provincial Qianfoshan Hospital, Jinan, China, Department of Endocrinology and Metabology, The Third Affiliated Hospital of Shandong First Medical University, Jinan, China

[2] Department of Endocrinology and Metabology, The Third Affiliated Hospital of Shandong First Medical University & Shandong Academy of Medical Sciences; Shandong Provincial Key Laboratory for Rheumatic Disease and Translational Medicine, The First Affiliated Hospital of Shandong First Medical University & Shandong Provincial Qianfoshan Hospital, Jinan, China

[3]Teaching and Research Section of Internal Medicine, College of Medicine, Shandong University of Traditional Chinese Medicine, Jinan, China

[4]Department of rehabilitation medicine, The Second Affiliated Hospital of Shandong University of Traditional Chinese Medicine, Jinan, China

[5]Cheeloo College of Medicine, Shandong University, Jinan, China

*Correspondence:

Zhongwen Zhang

zhangzhongwen@sdu.edu.cn

Shaohong Yu

sutcm2006@163.com

†These authors contributed equally.

Lead contact Further information and requests for resources and reagents should be directed to and will be fulfilled by the lead contact, Zhongwen Zhang (zhangzhongwen@sdu.edu.cn)

Abstract

Objective: To determine the efficacy and potential protective mechanism of canagliflozin combined with aerobic exercise in treating chronic heart failure (CHF).

Methods: Isoproterenol was injected into rats to create CHF models. The rats were then subsequently divided into saline, canagliflozin (3 mg/kg/d), aerobic exercise training, and canagliflozin combined with aerobic exercise training.

Results: Compared to the CHF group, the canagliflozin combined with the aerobic exercise group had superior ventricular remodelling and cardiac function. In rats treated with canagliflozin combined with aerobic exercise, the expression of cytochrome P450 (CYP) 4A3, CYP4A8, COL1A1, COL3A1, and FN1 reduced, while the expression of CYP26B1, ALDH1A2, and CYP1A1 increased significantly. Additionally, canagliflozin combined with aerobic exercise decreased the phosphorylation of AKT and ERK1/2.

Conclusion: Canagliflozin combined with aerobic exercise has a positive effect on the development of CHF via regulation of retinol metabolism and AKT/ERK signaling pathway.

Key words: Chronic heart failure; Aerobic exercise; Canagliflozin; Myocardial fibrosis; Retinol metabolism signalling pathway

Introduction

Chronic heart failure (CHF), the most prevalent form of cardiovascular illness, is a global health issue with a high death and morbidity rate[1]. The disease affects about 2% of the adult population worldwide, and the 5-year mortality rate is estimated to be between 45-60%;[2]. CHF is a complex condition characterized by a cardiac muscle's inability to maintain blood supply to peripheral tissues, resulting in decreased systemic energy metabolism[3]. Multiple studies have demonstrated that regulating cardiac energy metabolism is critical for treatment[4,5]. The β-oxidation of fatty acids in the mitochondria satisfies the heart's high energy requirements. Oliveros *et al*. observed previously observed that a vitamin A deficit paired antioxidant defenses, promoted lipid peroxidation in the adult rat heart, and altered aortic lipid metabolism[6]. The peroxisome proliferator-activated receptor (PPAR) is a ligand-activated nuclear transcription factor[7]. PPAR modulates fatty acid oxidation (FAO) and mitochondrial bioenergetics, suppresses myocardial remodeling and fibrosis, and improves HF[8]. Consequently, we must investigate new techniques for enhancing cardiac function by ameliorating abnormalities of cardiac energy metabolism, preventing cardiac remodeling and fibrosis, and thereby preventing or postponing the advancement of heart failure.

Canagliflozin, an inhibitor of sodium-glucose cotransporter 2 (SGLT-2), has been demonstrated to benefit HF with a lower ejection fraction[9]. SGLT-2 inhibitors (canagliflozin, etc.) for CHF patients, improve quality of life, and reduce mortality, morbidity, and readmission rates[10]. In diabetic and nondiabetic subjects, canagliflozin treatment significantly reduced the risk of cardiovascular death, myocardial infarction, and hospitalization for hypertension.[11]. In addition, SGLT-2 inhibitors can improve fatty acid metabolism and utilize ketone bodies to create mitochondrial energy, so enhancing the aerobic metabolism of skeletal muscle, inhibiting anaerobic metabolism, and enhancing aerobic exercise capacity[12]. Canagliflozin has

been demonstrated to decrease myocardial glucose metabolism, enhance myocardial fatty acid metabolism, and increase circulation of ketone bodies[13], thereby ameliorating heart failure via modifying myocardial energy metabolism and oxidative stress[14].

Aerobic exercise training is associated with improved aerobic capacity, cardiovascular function and metabolic regulation [15]. In patients with CHF, aerobic exercise positively benefits cardiovascular function, myocardial metabolism and antioxidant status[16]. Additionally, it can effectively reverse ventricular remodeling in heart failure, enhance aerobic capacity and maximal oxygen absorption[17]. The proposed mechanisms of aerobic exercise in the therapy of CHF include increased energy expenditure and improved metabolic function. Tomas *et al.* demonstrated that moderate-intensity aerobic exercise boosted mitochondrial respiration, ATP levels, and cardiac function in rats with CHF[18]. Also, aerobic exercise has been shown to stimulate the release of irisin in cardiomyocytes, thereby enhancing cardiomyocyte metabolism, preserving mitochondrial function, and increasing energy expenditure[19].

The 2021 Canadian Heart Failure Guidelines highlight the combination of prescribed medications (SGLT-2 inhibitors, beta-blockers, etc.) and nonpharmacological therapy for the treatment of CHF[10,20]. Based on canagliflozin medication, combined aerobic exercise may be more beneficial in treating CHF, but the particular effect and molecular mechanism remain unknown. This study was designed to examine the efficacy and potential protective mode of action of canagliflozin combined with aerobic exercise in the treatment of CHF.

Materials and Methods

2.1. Experimental animals

Male Sprague Dawley (SD) rats of eight weeks of age were acquired from Beijing Weitong Lihua Laboratory Animal Technology Co., Ltd. and animal experiments were conducted in the

SPF animal room of the First Affiliated Hospital of Shandong First Medical University (License number: SCXK Beijing 2016-0006). Before the experiment, the rats were housed for two weeks under standard temperature (21–23°C) and humidity (40–60 %) conditions with free access to food and drink. The care and use of laboratory animals conformed to the Guide for the Management and Use of Laboratory Animals, and the Animal Experimentation Committee of the First Affiliated Hospital of Shandong First Medical University granted ethical and scientific approval (2020S014).

2.2. Experimental protocol

70 rats were randomly assigned to two groups: the saline-treated control group (n = 6) and the CHF group (n = 64).As previously stated[21], the isoproterenol (ISO)-induced rat models of CHF were created. For ten days, rats were injected intra-peritoneally with a 5 mg/kg/d isoproterenol solution. Animals that have died were excluded from the study. After establishing the model, 24 rats in the CHF group survived and were randomized into four groups: the ISO+CA group (n = 6, oral administration of canagliflozin 3 mg/kg/d), the ISO+AE group (n = 6, aerobic exercise training on a small animal multitrack treadmill), the ISO+AE+CA group (n = 6, simultaneous oral administration of canagliflozin and aerobic exercise training), and the ISO group (n = 6, oral administration of equal amounts of normal saline).

Regarding the study by HIRA *et al.*[22], canagliflozin (Merck Serono, Beijing, China) was supplied through gavage, and the medication dose was established to be 3 mg/kg/d for 4 weeks. The aerobic exercise program is based on the design of Bedford *et al.*[23]. Every day, rats completed 5 to 10 minutes of warm-up exercise (speed 5 m/min, incline 0°), after which the speed was increased to 12 m/min and the elevation was altered to 5° (equivalent to 45 percent VO2max). On days 1, 2, and 3, the running time was 15, 30, and 45 minutes, respectively, and on day 4, the running time was increased to 60 minutes. The aerobic exercise was performed

six times each week for four weeks. The study excluded rats who refused to run steadily on the treadmill. After four weeks, the rats were anesthetized with 2% sodium pentobarbital (40 mg/kg) and sacrificed. Blood was obtained from the femoral artery, centrifuged to collect serum, and then stored at −80°C for ELISA. Cardiac tissue samples taken from the mid LV (2.5 mm above the apex) of the heart were fixed with 4% paraformaldehyde for histopathological analysis and immunohistochemical staining, and the remaining LV tissues were stored at −80 °C for western blot assay and qPCR analysis.

2.3. Echocardiographic assessment

Echocardiography was performed one day before the ISO injection, one day after the ISO injection, and four weeks after the drug and exercise interventions. To alleviate pain and anxiety, rats were sedated with 1.5% isoflurane and placed in the supine position. Left ventricular ejection fraction (LVEF) and left ventricular fractional shortening (LVFS) were the key parameters measured. Parameters such as the left ventricular end of systole volume (LVESV), left ventricular end of diastole volume (LVEDV), left ventricular internal diameter at end-systole (LVIDs), left ventricular internal diameter at end-diastole (LVIDd), left ventricular posterior wall diastole (LVPWd), left ventricular posterior wall systole (LVPWs), left ventricular anterior wall diastole (LVAWd) and left ventricular anterior wall systole (LVAWs) were obtained from the 2D-guided M-mode measurements by software of the Vevo 3100 (VisualSonics Inc, Toronto, Ontario, Canada). The values of LVFS and LVEF were calculated by the Vevo LAB software. Carry out three measurement analyses and take the average value of the three analyses.

2.4. Histopathological examination

After immobilizing myocardial tissues with 4% paraformaldehyde for at least 48 hours, paraffin sections were prepared. These sections were stained with hematoxylin-eosin (HE) and Masson trichrome to evaluate histopathological alterations and collagen deposition, then photographed at a magnification of 40×. Using Image-Pro Plus 6.0, the collagen volume fraction (collagen area/total area × 100%) was calculated.

2.5. Immunohistochemistry

The hearts were submerged in paraformaldehyde at a concentration of 4% and embedded in paraffin. Cross-sections of the heart were dewaxed, heated for antigen retrieval, treated with 3 percent hydrogen peroxide to inhibit endogenous peroxidase activity, and then blocked with 4 percent bovine serum albumin. The sections were then treated overnight at 4°C with the primary antibodies collagen I (COL1) (Abcam, 1:150), collagen III (COL3) (Abcam, 1:700) and Fibronectin (FN1) (Abcam, 1:1000). The slices were treated with the appropriate secondary antibodies, and the positive staining was detected with diaminobenzidine (DAB) and counterstained with hematoxylin before being studied under a 40-magnification electron microscope. Image Pro Plus 6.0 software was used to quantify every image.

2.6. RNA sequencing (RNA-seq)

Total RNA was extracted from the apical tissue using the RNeasy Mini Kit (250) Qi-agen#74106 kit, and three biological replicates in the Control, ISO, ISO+CA and ISO+AE+CA groups were used for quality inspection and RNA quantification. Strand-specific libraries were prepared following depletion of ribosomal RNA and sequenced on an Illumina NovaSeq 6000 instrument using the paired-end sequencing chemistry.

The raw off-machine data were first processed to obtain high-quality sequences, and then the high-quality sequences were aligned to reference genes, and the results were quantified for

transcriptome expression. Differentially expressed genes were calculated and differentially screened by Fragments Per Kilobase per Million (FPKM), etc. Screening criteria: P value<0.05 and the fold change (FC) is 2 times up (FC≥2) or 2 times down (FC≤2) 0.5) and eliminated the differentially expressed genes with FPKM less than 1 in each group. Visual analysis of sequencing results using R language and bioinformatics online tools (http://www.bioinformatics.com.cn/). The STRING 11.5 database[24] (https://cn.string-db.org) contains genes with distinct expressions. After hiding unconnected nodes, platform and protein-protein interaction (PPI) networks were obtained. To further examine the PPI network, the Molecular Complex Detection (MCODE) [25]tool of Cytoscape 3.7.1[26] (http://cytoscape.org/) was utilized. Gene Ontology (GO) functional analysis and Kyoto Encyclopedia of Genes and Genomes (KEGG) enrichment analysis were performed using Metascape[27] (https://metascape.org/), and bioinformatics online tools and Cytoscape 3.7.1 software were utilized for data visualization.

2.7. Western blot analysis

Protein lysates from heart tissue were separated by 10% SDS-PAGE and then transferred to PVDF membranes (EMD Millipore, Billerica, MA, USA). Membranes were incubated overnight at 4 ˚C with the following primary antibodies: β-tubulin (1:1,000; 10068-1-AP; Proteintech), AKT (1:1,000; cat. no. ab32505; Abcam), phosphorylated AKT (p-AKT) (1:1,000; cat. no. ab192623; Abcam), ERK1/2 (1:1,000; cat. no. ab184699; Abcam), and phosphorylated ERK1/2 (1:1,000; cat. no. ab201015; Abcam). The membranes were cleaned and incubated with the appropriate secondary antibody (1:10000) at room temperature for one hour the following day. Using an ECL Chemiluminescence Kit, blots were seen (servicebio, Wuhan, China). Using the FluorChem E imaging equipment, the protein bands were semi quantified (ProteinSimple, San Francisco, CA, USA). Using an image analysis system, protein band

densities were assessed and expressed as ratios to AKT or ERK1/2.

2.8. Quantitative reverse transcription-PCR analysis

Total RNA was extracted using TRIzol reagent (Genstar, Beijing, China) according to the manufacturer's protocol, and cDNA was obtained by reverse transcription reaction with *mRNA* utilizing an AccuPower RT PreMix kit (Accurate Biology, Hunan, China). Quantitative real-time PCR (qPCR) was used to determine the *mRNA* levels of collagen 1 alpha 1 (COL1A1), collagen 3 alpha 1 (COL3A1), FN1, cytochrome P450 (CYP) 1A1, CYP2C23, CYP4A8, CYP4A3, CYP26B1, Aldehyde oxidase 1 (AOX1), Aldehyde dehydrogenase 1 family member A2 (ALDH1A2). As an internal control, β-actin was used to calculate relative expression. The relative RNA concentration was determined using the $2^{-\Delta\Delta ct}$ method.

2.9. Enzyme-linked immunosorbent assay (ELISA) analysis

After four weeks of intervention, blood samples from rats were collected. ELISA Kits were used to determine the serum concentrations of N-terminal pro-B-type natriuretic peptide (NT-pro BNP) (Shanghai Enzyme-linked Biotechnology Co., Ltd.) according to the manufacturer's instructions.

2.10. Statistical analysis

GraphPad Prism 8 software (GraphPad, SanDiego, CA, USA) was used to analyze the data, and the results are presented as mean ± standard errors of mean (SEM). For multivariate comparisons between groups, a two-way ANOVA followed by the Turkey post–hoc test was used. $p<0.05$, $p<0.01$, $p<0.001$ and $p<0.0001$ were considered to be statistically significant.

Results

3.1. Canagliflozin combined with aerobic exercise improved ISO-induced cardiac dysfunction

To investigate the effect of canagliflozin combined with aerobic exercise on CHF, cardiac function was assessed using echocardiography. After 10 days of ISO administration, the levels of LVEF ($P < 0.001$) and LVFS ($P < 0.001$) in the ISO group were significantly lower than in the control group, indicating that the CHF rat model was successfully established. LVEF and LVFS levels were significantly higher in the ISO+CA group (LVEF, $P < 0.05$; LVFS, $P < 0.05$), the ISO+AE group (LVEF, $P < 0.05$; LVFS, $P < 0.05$), and the ISO+AE+CA group (LVEF, $P < 0.01$; LVFS, $P < 0.01$). Moreover, compared to the ISO group, the levels of LVIDs ($P < 0.05$) and LVESV ($P < 0.05$) were significantly reduced in the ISO+AE+CA group but not in the ISO+CA group (LVIDs, $P = 0.21$; LVESV, $P = 0.21$). **(Figure 1(A, B), Table 1)**.

To further confirm the protective effect of canagliflozin combined with aerobic exercise on CHF, NT-pro BNP serum levels were measure[28]. Compared to the ISO group, the NT-pro BNP levels in the ISO+AE group ($P < 0.01$), the ISO+CA group ($P < 0.05$), and the ISO+AE+CA group ($P < 0.01$) were significantly lower **(Table 1)**. These results suggested that ISO impaired cardiac function and that canagliflozin intervention alone and in combination with aerobic exercise therapy improved ISO-induced cardiac insufficiency by enhancing myocardial contractility.

TABLE 1. Canagliflozin combined with aerobic exercise improved left ventricular function in ISO-induced rats.

Group	Control	ISO	ISO+AE	ISO+CA	ISO+CA+AE
LVPWd (mm)	2.64±0.47	2.33±0.12	2.42±0.26	2.28±0.16	2.46±0.17
LVPWs (mm)	3.31±0.35	3.35±0.26	3.56±0.35	3.76±0.17	3.92±0.23

LVAWd (mm)	2.74±0.22	2.05±0.21	2.23±0.13	2.17±0.15	2.49±0.20
LVAWs (mm)	4.04±0.06	2.71±0.20$^{\#\#}$	3.14±0.24	2.99±0.10	3.21±0.32
LVIDd (mm)	7.11±0.31	6.73±0.04	6.09±0.30	7.01±0.39	6.64±0.61
LVIDs (mm)	2.86±0.38	4.16±0.28$^{\#\#}$	2.67±0.25***	3.56±0.26	3.39±0.32*
LVEDV (ul)	272.20±29.05	248.80±7.02	159.40±18.84***	260.10±32.15	237.00±54.53
LVESV (ul)	60.15±11.05	111.40±18.51$^{\#\#}$	43.03±8.68***	74.01±10.62	56.47±13.57**

ISO: isoproterenol-treated group; ISO + AE: ISO + aerobic exercise group. ISO + CA: ISO + canagliflozin. ISO + AE + CA: ISO + aerobic exercise + canagliflozin. LVPWd: left ventricular posterior wall thickness at end-diastole. LVPWs: left ventricular posterior wall thickness at end systole. LVAWd: left ventricular anterior wall diastole. LVAWs: left ventricular end systolic anterior wall thickness. LVIDd: left ventricular end-diastolic inner-dimension. LVIDs: left ventricular end-systolic inner-dimension. LVEDV: left ventricular end-diastolic volume. LVESV: left ventricular end-systolic volume. The results are expressed as mean ± SEM of n = 5 per group. Significance: # $P < 0.05$ vs. control group; ## $P < 0.01$ vs. control group; #### $P < 0.0001$ vs. control group; * $P < 0.05$ vs. ISO group; **P <0.01 vs. ISO group; *** $P < 0.001$ vs. lSO group. Data are represented as mean ±SEM.

3.2. Canagliflozin combined with aerobic exercise can improve ISO-induced ventricular remodeling

We used HE and Masson trichrome staining to determine the effects of canagliflozin in conjunction with aerobic exercise on ISO-induced pathological morphology and collagen fiber deposition in rat hearts.

Figure 2(A) demonstrates that the cardiomyocytes in the ISO group were significantly sparse and hypertrophied, the myocardial fibers were broken and disorganized. With a relatively neat arrangement of myocardial fibers, the pathological histological changes of the rats in the ISO+AE+CA group were improved. As depicted in **Figure 2(B, F)**, Masson trichrome staining revealed that collagen fiber deposition was significantly elevated in the ISO group ($P < 0.0001$) compared to the control group. The deposition of collagen fibers was significantly reduced in the ISO+AE group ($P < 0.001$), the ISO+CA group ($P < 0.01$), and

the ISO+AE+CA group ($P < 0.0001$) compared to the ISO group. Intervention with canagliflozin alone or combined with aerobic exercise therapy improved myocardial pathological changes and decreased collagen fiber deposition.

To examine the potential modulating effect of canagliflozin combined with aerobic exercise therapy on myocardial fibrosis, the immunohistochemical expression of the fibrosis markers COL1, COL3 and FN1 was measured. As shown in **Figure 2(C, D, E)**, quantitative image analysis revealed a significant increase in COL1 ($P < 0.0001$), COL3 ($P < 0.0001$) and FN1 ($P < 0.05$) expression in the ISO group compared to the control group. Compared with the ISO group, the expression of COL1, COL3 and FN1 in the ISO+AE group (COL1, $P < 0.01$; COL3, $P < 0.01$; FN1, $P < 0.01$), ISO+CA group (COL1, $P < 0.001$; COL3, $P < 0.05$; FN1, $P < 0.05$) and ISO+AE+CA group (COL1, $P < 0.001$; COL3, $P < 0.001$; FN1, $P < 0.05$) were significantly reduced.

RT-PCR was used to confirm the differential expression of genes associated with fibrosis. As shown in **Figure 2(G)**, The *mRNA* levels of COL1A1 ($P < 0.0001$), COL3A1 ($P < 0.01$) and FN1 ($P < 0.001$) were significantly up-regulated in the ISO group compared with the control group, whereas the expression of COL1A1, COL3A1 and FN1 genes were down-regulated in the ISO+AE group (COL1A1, $P < 0.001$; COL3A1, $P < 0.001$; FN1 $P < 0.05$), the ISO+CA group (COL1A1, $P < 0.001$; COL3A1, $P < 0.05$, FN1< 0.05), and the ISO+AE+CA group (COL1A1, $P < 0.0001$; COL3A1, $P < 0.0001$; FN1, $P < 0.01$), compared with the ISO group. These results suggested that both canagliflozin intervention and combined aerobic exercise training can reduce myocardial fibrosis.

3.3. Canagliflozin combined with aerobic exercise attenuated ISO-induced CHF in rats mainly by the retinol metabolism signaling pathway.

The cardiac transcriptome of the control, ISO, ISO+CA and ISO+AE+CA groups were profiled

and qPCR was used to validate the sequencing data. We focused our analysis on the sequencing results of the ISO group versus the Control group and ISO+AE+CA group versus the ISO group. RNA-seq detected 18,713 genes in the apical tissue of the ISO groups and Control group, there were 19,091 genes in the apical tissue of the canagliflozin combined with aerobic exercise treatment and ISO groups, with 152 differentially expressed genes, including 51 up-regulated and 101 down-regulated genes (**Figure 3**). From the PPI network, an MCODE module consisting of 6 targets were identified, which may play more significant regulatory roles (**Figure 4(A)**).

Figure 4(B) depicts the biological process items from the differentially expressed genes' GO analysis. Down-regulated genes were associated with response to vitamin A, retinoic acid metabolic process, positive regulation of icosanoid secretion and regulation of icosanoid secretion. Up-regulated genes were predominantly involved in the collagen metabolic process, response to organophosphorus, response to retinoic acid and diterpenoid metabolic process. Most involved in the retinol metabolism, PI3K-Akt signaling pathway, AGE-RAGE signaling pathway in diabetic complications and TNF signaling pathway, according to the KEGG pathway enrichment analysis (**Figure 4(C)**). Intriguingly, the majority of the differentially expressed genes were enriched in the retinol metabolism pathway, and the GO analysis also included responses to vitamin A and the retinoic acid metabolic process. Therefore, we hypothesized that the combination of canagliflozin and aerobic exercise could improve CHF primarily via the retinol metabolism pathway.

Based on the results of the KEGG pathway enrichment analysis, a target pathway network was constructed using Cytoscape 3.7.1 (**Figure 4(D)**). CYP4A3, CYP4A8, ALDH1A2, CYP26B1, CYP1A1 and AOX1 in the protein functional module were enriched in the retinol metabolic pathway, consequently, these six targets were deemed essential for further qPCR

validation. As shown in **Figure 5(A, B)**, relative to the control group, the *mRNA* levels of CYP4A3 ($P < 0.05$), CYP4A8 ($P < 0.0001$) and AOX1 ($P < 0.0001$) in the ISO group were significantly up-regulated, while ALDH1A2 ($P < 0.01$), CYP26B1 ($P < 0.05$) and CYP1A1 ($P < 0.01$) were significantly down-regulated. By treating with canagliflozin alone (CYP4A3, $P < 0.05$; CYP4A8, $P < 0.0001$), aerobic exercise alone (CYP4A3, $P < 0.05$; CYP4A8, $P < 0.001$), or in combination with aerobic exercise (CYP4A3, $P < 0.0001$; CYP4A8, $P < 0.0001$), the *mRNA* levels of CYP4A3 and CYP4A8 were significantly down. In addition, canagliflozin combined with aerobic exercise significantly upregulated the levels of ALDH1A2 ($P < 0.001$), CYP1A1 ($P < 0.05$) and CYP26B1 ($P < 0.001$). As expected, the qPCR results were largely congruent with those of RNA-seq, demonstrating the precision of the high-throughput RNA-seq results.

Canagliflozin combined with aerobic exercise exerted the protective effect against CHF by Inhibiting the activation of the AKT/ERK signaling pathway

AKT/ERK signaling pathways that are activated can exacerbate myocardial fibrosis [29-31]. Our preliminary sequencing results indicated that the biological process analysis of the down-regulated genes includes components that regulate the activity of protein kinase. To determine whether the activation was inhibited by the combination of canagliflozin and aerobic exercise, the phosphorylation status of the AKT and ERK signaling pathway was determined using Western blotting. The basal levels of AKT and ERK1/2 did not differ significantly between groups. However, compared to the control group, the p-AKT/AKT ratio ($P < 0.0001$) and p-ERK1/2/ERK1/2 ratio ($P < 0.0001$) were elevated in the ISO group indicating that ISO stimulation activated the AKT/ERK signaling pathway in rats. Compared to the ISO group, the p-AKT/AKT ratio and the p-ERK1/2/ERK1/2 ratio were significantly decreased in the ISO+CA group (p-AKT/AKT, $P < 0.01$; p-ERK1/2/ERK1/2, $P < 0.001$), ISO+AE group (p-

AKT/AKT, $P < 0.01$; p-ERK1/2/ERK1/2, $P < 0.001$) and a combination of both (p-AKT/AKT, $P < 0.0001$; p-ERK1/2/ERK1/2, $P < 0.001$). These findings supported the conclusion that canagliflozin treatment alone or in conjunction with aerobic exercise may be cardioprotective by inhibiting AKT/ERK pathway activation **(Figure 6)**.

Discussion

CHF is a complex end-stage of multiple cardiovascular diseases caused by diastolic or systolic heart dysfunction[32]. Given that the pathogenesis of CHF is associated with a variety of factors, including neurohormonal activation, ventricular remodeling, and disturbances in energy metabolism [2], multi-target and multi-pathway therapy may be more effective for the treatment of CHF. In the present study, we first confirmed that canagliflozin combined with aerobic exercise treatment could improve cardiac function and myocardial fibrosis. Incorporating network pharmacology and whole-transcriptome sequencing, we found that canagliflozin combined with aerobic exercise exerts a protective effect in rats with CHF primarily by modulating the retinol metabolic pathway. The levels of ALDH1A2, CYP26B1 and CYP1A1 on this pathway were significantly up-regulated, while the levels of CYP4A3 and CYP4A8 were down-regulated. In addition, in vivo validation experiments have further demonstrated the cardioprotective effect of canagliflozin in combination with aerobic exercise by inhibiting the activation of AKT/ERK pathways.

Accumulating evidence indicates that pharmacological targeting of the energy metabolic pathways has emerged as a novel therapeutic approach for enhancing cardiac function in a failing heart[33]. Vitamin A (retinol) and its derivatives regulate fundamental biological processes such as development, differentiation, and metabolism[34], and lipid metabolism was significantly altered in the hearts of retinol-deficient rats. Retinol deprivation is associated with a high level of PPAR expression[6]. PPARs play a crucial role in fatty acid metabolism in the heart and are

342 implicated in the pathogenesis of cardiac hypertrophy and HF. Retinoic acid (RA) is a retinoid
343 derivative that inhibits the progression of myocardial remodeling by modulating the expression
344 of components of the renin-angiotensin system, thereby controlling left ventricular hypertrophy
345 and fibrosis[35,36]. ALDH1A2 is the primary form of RALDHs involved in early embryonic and
346 cardiac development[37]. ALDH1A2 encodes retinal dehydrogenase type 2, which is required for
347 the conversion of dietary retinol to retinoic acid[38]. In cells, retinol is initially reversibly
348 oxidized to retinal[39], and then retinal is irreversibly converted to retinoic acid. In the GO
349 analysis, responses to retinoic acid and vitamin A were also mentioned. Thus, the retinol
350 metabolic pathway may be critical for the regulation of cardiac energy metabolism in CHF rats
351 when canagliflozin and aerobic exercise are intervened simultaneously.

352 In this study, the key retinol metabolic pathway indicators CYP4A3, CYP4A8, CYP26B1
353 and CYP1A1 are members of the cytochrome The cytochrome P450 (P450) family. It is well
354 established that P450 ω-hydroxylases, particularly CYP4A, are involved in Cardiovascular
355 diseases (CVD)[40]. In failing and hypertrophied hearts, CYP4A subfamily expression was found
356 to be upregulated[41]. Previous research has demonstrated that sustained ISO stimulation of
357 cardiomyocytes increases the expression of CYP4A3, a major CYP450 ω-hydroxylase that
358 generates 20-hydroxyeicosatetraenoic acid (20-HETE) in a time-dependent manner with
359 adverse cardiovascular effects.[40]. Inhibition of CYP450 ω-hydroxylase decreased 20-HETE
360 production, protecting cells from ISO-induced apoptosis[42]. Consistent with previous findings,
361 the present study indicates that canagliflozin in combination with aerobic exercise significantly
362 decreased the levels of CYP4A3 and CYP4A8, leading to improvement in heart failure.

363 The fibrotic response of the heart is a dynamic process in which transforming growth
364 factor-β (TGF-β1) is upregulated and activate downstream signals, including AKT and
365 ERK[29,43]. And the PI3K-Akt signaling pathway was downstream of TGF-β1, which

significantly stimulated PI3K-Akt signaling pathway activity in cardiac fibroblasts[43]. PI3K is an enzyme that can be activated and catalyze the conversion of phosphatidylinositol diphosphate (PIP2) in the cell membrane to phosphatidylinositol triphosphate (PIP3). AKT is an important cell signaling protein, which is activated by binding to PIP3[44]. Activated AKT further regulates various biological processes, including cell growth, survival, and metabolism. ERK is another important signaling protein. It is a member of the mitogen-activated protein kinase (MAPK) family, involved in the regulation of cell proliferation, differentiation and survival[45]. TGF-β1 is a cytokine that plays an important role in cell growth, differentiation, migration, and matrix synthesis[46]. TGF-β1 signaling mainly conducts signals by binding to TGF-β receptors on the cell surface and activating Smad proteins. Activated Smad proteins further regulate gene transcription and cellular function. In cell signaling, the PI3K / AKT-ERK signaling pathway and the TGF-β1 signaling pathway can interact. It was shown that PI3K / AKT signaling can promote the production and release of TGF-β1, while also modulate the activation and effects of TGF-β1 signaling[47]. Moreover, TGF-β1 signaling can also affect cell growth and survival by regulating the activation of the PI3K / AKT-ERK signaling pathway[48]. Li *et al*. discovered that inhibiting AKT/ERK signaling pathways could ameliorate ISO-induced myocardial fibrosis in mice[29,49,50]. Activation of ERK signaling has been shown to induce cardiac hypertrophy, whereas inhibition of ERK consistently reduces cardiac hypertrophy and fibrosis[51]. Consistent with previous research, we found that the combination of canagliflozin and aerobic exercise significantly decreased the *mRNA* levels of COL1A1, COL3A1, and FN1 and inhibited AKT and ERK phosphorylation. These results suggest that inhibiting the AKT/ERK signaling pathway can ameliorate myocardial fibrosis in rats with ISO.

Conclusions

This study demonstrated that the combination of canagliflozin and aerobic exercise can reduce fibrosis and improve cardiac function by regulating retinol metabolism and the AKT/ERK signaling pathway, thereby exerting a significant protective effect against the development of CHF. Our results provide a rational basis for future clinical studies of canagliflozin in non-diabetic kidney disease. Further understanding of the mechanism of canagliflozin regulation has clinical relevance and provides important insights into the cardio-protective actions of canagliflozin **(Figure 7)**.

Clinical Perspective

1. Chronic heart failure, the most prevalent form of cardiovascular illness, is a global health issue. Canagliflozin treatment significantly reduced the risk of cardiovascular death, myocardial infarction and hospitalization for HF in both diabetic and non-diabetic subjects. Heart Failure Guidelines highlight the combination of prescribed medications (SGLT-2 inhibitors) and nonpharmacological therapy for the treatment of CHF. Canagliflozin combined with aerobic exercise may be more beneficial in treating CHF, but the particular effect and molecular mechanism remain unknown.

2. The combination of canagliflozin and aerobic exercise can reduce fibrosis and improve cardiac function by regulating retinol metabolism and the AKT/ERK signalling pathway, thereby exerting a significant protective effect against the development of CHF.

3. Our results provide a rational basis for future clinical studies of canagliflozin in non-diabetic kidney disease. Further understanding of the mechanism of canagliflozin regulation has clinical relevance and provides important insights into the cardio-protective actions of canagliflozin.

Limitations of the study

Although this study provides an in-depth study of the protective role of canagliflozin combined with aerobic exercise in the development of heart failure, there are several limitations. This study used a mouse model, so the findings may not be directly applicable to humans. Further clinical studies and human trials are still necessary to verify the efficacy and safety of this combination therapy in human patients.

Acknowledgements

This work was supported by the Natural Science Foundation of China [no. 82000788]; Chinese Postdoc-toral Science Foundation [2021M702040]; Key Research & Development Plan of Shandong Province [no. 2018GSF118176]; Guangdong Basic and Applied Basic Research Foundation [no. 2019A1515110023]; Natural Science Foundation of Shandong Province [no. ZR2016HQ26]; the Bethune-Merck's Diabetes Research Foundation [no. B-0307-H-20200302, G2016014]; Medicine and Health Science and Technology Development Plan of Shandong Province [no. 2018WS201]; and Science and technology plan of Shandong Provincial University [no. J16LK09].

Author Contributions

ZZW and YSH contributed to study conception and preparation of the manuscript. FH, YZD and WXY contributed to study conception and design, SHL and DBY drafted the manuscript and gave final approval of the version to be sent.

Conflicts of Interest

The authors declare that they have no conflict of interest.

Resource availability

Lead contact Further information and requests for resources and reagents should be directed to and will be fulfilled by the lead contact, Zhongwen Zhang (zhangzhongwen@sdu.edu.cn)

Material availability This study did not generate any new unique reagents.

Data availability All relevant data for this study are available from the corresponding authors (accession number GSE225149). This paper does not report original code. Any additional information required to reanalyze the data reported in this paper is available from the lead contact upon request. The data used to support the findings of this study are available from the corresponding author upon request.

FIGURE 1. Effects of canagliflozin combined with aerobic exercise on echocardiographic variables in rats induced by ISO. (A) The representative images of echocardiography in different groups. (B) The quantitative results of echocardiography. (C) The expression level of NT-pro BNP. Data are shown as the mean ± SEM of n = 5 per group. Significance: ### $P < 0.001$ vs. control group; #### $P < 0.0001$ vs. control group; * $P < 0.05$ vs. ISO group; ** $P < 0.01$ vs. ISO group. ISO, isoproterenol-treated group; ISO + AE, ISO + aerobic exercise group. ISO + CA, ISO + canagliflozin; ISO + AE + CA, ISO + aerobic exercise + canagliflozin; LVEF, left ventricular ejection fraction; LVFS, left ventricular fractional shortening; NT-pro BNP, N-terminal pro-B-type natriuretic peptide. Data are represented as mean ±SEM.

FIGURE 2. Effects of canagliflozin combined with aerobic exercise on ventricular remodelling in rat heart tissue. (A) Representative images of HE staining of left ventricular tissue in different groups (Microscope magnification 10X, scale bar indicates 200μm; Microscope magnification 40X, scale bar indicates 50μm). (B) Representative images of Masson trichrome staining of left ventricular tissue in different groups, (Microscope magnification 10X, scale bar indicates 200μm; Microscope magnification 40X, scale bar indicates 50μm). (C-E) Immunohistochemical analysis of collagen I, collagen III and fibronectin protein in heart cross sections of different groups (Microscope magnification 40X, scale bar indicates 50μm). (F) The quantitative analysis of collagen deposition and percentage area of collagen I, collagen III and fibronectin. (G) The gene expression levels of COL1A1, COL3A1 and FN1 were detected by qPCR. The internal reference was β-actin. Data are shown as the mean ± SEM of n = 5-6 per group. Significance: ### $P < 0.001$ vs. control group; #### $P < 0.0001$ vs. control group; *** $P < 0.001$ vs. ISO group; **** $P < 0.0001$ vs. lSO group. ISO, isoproterenol-treated group; ISO + AE, ISO + aerobic exercise group; ISO + CA, ISO + canagliflozin; ISO + AE + CA, ISO + aerobic exercise + canagliflozin; HE, hematoxylin-eosin; COL1, Collagen I; COL3, Collagen III; FN1, fibronectin. Data are represented as mean ±SEM.

FIGURE 3. RNA-seq was performed to detect genome-wide transcriptomes and identify differentially expressed genes. (A) Volcano plot of differential genes from the ISO group and the Control group identified through RNA-seq. The abscissa is log2 (fold change), and the vertical coordinate is the negative logarithm of the value of Q with a base of 10, i.e. -log10 (Q). The larger the value, the more significant the difference. (B) Scatter plot of differential genes. The horizontal and vertical coordinates represent the samples from the ISO group and the ISO+AE+CA group, respectively. The red indicates the up-regulated differential genes in the ISO+AE+CA group relative to the ISO group and the blue indicates the down-regulated differential genes in the AE+CA group relative to the ISO group, and the grey indicates genes that are not different between the two groups. (C)Venn diagram. The orange section indicates differential genes from the ISO group and the Control group targets, and the green section indicates differential the ISO group and the ISO+AE+CA group targets. One hundred and fifty-two targets in the middle overlapping section are common targets. (D) Histogram of differential genes. (E) Heat map of differential genes. Each row represents a differential gene, each column represents the same rat sample, and each group has 3 replicates.

FIGURE 4. Enrichment analysis of the targets of canagliflozin combined with aerobic exercise in treating CHF. (A) PPI network. A total of 120 target proteins and 258 interacting edges are in the network. The sizes and colours of the nodes are illustrated from big to small and blue to green in descending order of degree values. (B) GO functional analysis. Biological process items in GO analysis enriched for up-regulated and down-regulated genes respectively. (C) KEGG pathway enrichment analysis. The sizes of the bubbles were illustrated from big to small in descending order of the number of potential targets involved in the pathways. (D) Target-pathway network. A total of 36 nodes and 54 edges are in the network. The middle square nodes represent targets on the pathway, the red nodes represent key targets, and 12 blue V-shapes represent pathways. The sizes of the square node were illustrated from big to small in descending order of degree values. 54 edges represent the interaction relationship between components, targets, and pathways. CHF, chronic heart failure; PPI, protein-protein interaction; GO, Gene Ontology; KEGG, Kyoto Encyclopaedia of Genes and Genomes.

FIGURE 5. Effects of canagliflozin combined with aerobic exercise on retinol metabolic pathways and indicators of fibrosis. (A) The gene expression levels of CYP4A3, CYP4A8 and CYP1A1 were detected by transcriptome sequencing and qPCR. The internal reference was β-actin. (B) The gene expression levels of CYP26B1, ALDH1A2 and AOX1 were detected by transcriptome sequencing and qPCR. The internal reference was β-actin. Data are shown as the mean ± SEM of n = 6 per group. Significance: # $P < 0.05$ vs. control group; ## $P < 0.01$

vs. control group; #### $P < 0.0001$ vs. control group; * $P < 0.05$ vs. ISO group; ** P < 0.01 vs. ISO group; *** $P < 0.001$ vs. ISO group; **** P < 0.0001 vs. ISO group. ISO, isoproterenol-treated group; ISO + AE, ISO + aerobic exercise group; ISO + CA, ISO + canagliflozin; ISO + AE + CA, ISO + aerobic exercise + canagliflozin; ELISA, enzyme linked immunosorbent assay; qPCR, reverse transcription-polymerase chain reaction. Data are represented as mean ±SEM.

FIGURE 6. Effects of canagliflozin combined with aerobic exercise on the AKT/ERK signalling pathway in rats. The protein expression levels of AKT, p-AKT, ERK1/2 and p-ERK1/2 were determined by western blot. (A) The protein expression levels of AKT, p-AKT, ERK1/2 and p-ERK1/2 in heart tissues, and β-tubulin was used as the internal standard. (B) The quantitative results were calculated by Image Lab software. Data are shown as the mean ± SEM of n = 3 per group. Significance: ## $P < 0.01$ vs. control group; ### $P < 0.001$ vs. control group; * $P < 0.05$ vs. ISO group; ** $P < 0.01$ vs. ISO group; *** $P < 0.001$ vs. lSO group; **** $P < 0.0001$ vs. lSO group. ISO, isoproterenol-treated group; ISO + AE, ISO + aerobic exercise group; ISO + CA, ISO + canagliflozin; ISO + AE + CA, ISO + aerobic exercise + canagliflozin; p-AKT, phosphorylated AKT; p-ERK1/2, phosphorylated ERK1/2. Data are represented as mean ±SEM.

FIGURE 7. The mechanism of aerobic exercise combined with canagliflozin therapy against ISO-induced CHF. Canagliflozin combined with aerobic exercise therapy modulates protein kinase activity. The combination therapy inhibited the activation of AKT/ERK signaling pathway, thereby improving myocardial fibrosis. Canagliflozin combined with aerobic exercise improved cardiac energy metabolism in CHF rats mainly through the retinol metabolic pathway. The combination significantly upregulated CYP1A1 levels to promote the conversion of retinol to retinoic acid, and it also improved myocardial fibrosis by regulating ALDH1A2 and CYP26B1 to maintain retinoic acid homeostasis. Meanwhile, the combination treatment reduced heart failure by downregulating CYP4A3 and CYP4A8 levels to reduce the production of 20-hydroxyeicosatetraenoic acid.

References

1. Wen, J., Zhang, L., Liu, H., Wang, J., Li, J., Yang, Y., Wang, Y., Cai, H., Li, R., and Zhao, Y. (2019). Salsolinol Attenuates Doxorubicin-Induced Chronic Heart Failure in Rats and Improves Mitochondrial Function in H9c2 Cardiomyocytes. Frontiers in pharmacology *10*, 1135. 10.3389/fphar.2019.01135.
2. Zhang, S., Liu, H., Fang, Q., He, H., Lu, X., Wang, Y., and Fan, X. (2021). Shexiang Tongxin Dropping Pill Protects Against Chronic Heart Failure in Mice via Inhibiting the ERK/MAPK and TGF-β Signaling Pathways. Frontiers in pharmacology *12*, 796354. 10.3389/fphar.2021.796354.
3. Wang, L., Gao, K., and Wang, D. (2018). Exercise training has restorative potential on myocardial energy metabolism in rats with chronic heart failure. Iranian journal of basic medical sciences *21*, 818-823. 10.22038/ijbms.2018.29294.7076.

4. Wu, D., Jian, C., Peng, Q., Hou, T., Wu, K., Shang, B., Zhao, M., Wang, Y., Zheng, W., Ma, Q., et al. (2020). Prohibitin 2 deficiency impairs cardiac fatty acid oxidation and causes heart failure. Cell death & disease *11*, 181. 10.1038/s41419-020-2374-7.
5. Bashir, A., Zhang, J., and Denney, T.S. (2020). Creatine kinase rate constant in the human heart at 7T with 1D-ISIS/2D CSI localization. PLoS One *15*, e0229933. 10.1371/journal.pone.0229933.
6. Vega, V.A., Anzulovich, A.C., Varas, S.M., Bonomi, M.R., Giménez, M.S., and Oliveros, L.B. (2009). Effect of nutritional vitamin A deficiency on lipid metabolism in the rat heart: Its relation to PPAR gene expression. Nutrition (Burbank, Los Angeles County, Calif.) *25*, 828-838. 10.1016/j.nut.2009.01.008.
7. Saibil, S.D., St Paul, M., Laister, R.C., Garcia-Batres, C.R., Israni-Winger, K., Elford, A.R., Grimshaw, N., Robert-Tissot, C., Roy, D.G., Jones, R.G., et al. (2019). Activation of Peroxisome Proliferator-Activated Receptors α and δ Synergizes with Inflammatory Signals to Enhance Adoptive Cell Therapy. Cancer research *79*, 445-451. 10.1158/0008-5472.Can-17-3053.
8. Khuchua, Z., Glukhov, A.I., Strauss, A.W., and Javadov, S. (2018). Elucidating the Beneficial Role of PPAR Agonists in Cardiac Diseases. International journal of molecular sciences *19*. 10.3390/ijms19113464.
9. Packer, M., Anker, S.D., Butler, J., Filippatos, G., Ferreira, J.P., Pocock, S.J., Carson, P., Anand, I., Doehner, W., Haass, M., et al. (2021). Effect of Empagliflozin on the Clinical Stability of Patients With Heart Failure and a Reduced Ejection Fraction: The EMPEROR-Reduced Trial. Circulation *143*, 326-336. 10.1161/circulationaha.120.051783.
10. McDonald, M., Virani, S., Chan, M., Ducharme, A., Ezekowitz, J.A., Giannetti, N., Heckman, G.A., Howlett, J.G., Koshman, S.L., Lepage, S., et al. (2021). CCS/CHFS Heart Failure Guidelines Update: Defining a New Pharmacologic Standard of Care for Heart Failure With Reduced Ejection Fraction. The Canadian journal of cardiology *37*, 531-546. 10.1016/j.cjca.2021.01.017.
11. Aragón-Herrera, A., Feijóo-Bandín, S., Otero Santiago, M., Barral, L., Campos-Toimil, M., Gil-Longo, J., Costa Pereira, T.M., García-Caballero, T., Rodríguez-Segade, S., Rodríguez, J., et al. (2019). Empagliflozin reduces the levels of CD36 and cardiotoxic lipids while improving autophagy in the hearts of Zucker diabetic fatty rats. Biochemical pharmacology *170*, 113677. 10.1016/j.bcp.2019.113677.
12. Takada, S., Sabe, H., and Kinugawa, S. (2022). Treatments for skeletal muscle abnormalities in heart failure: sodium-glucose transporter 2 and ketone bodies. American journal of physiology. Heart and circulatory physiology *322*, H117-h128. 10.1152/ajpheart.00100.2021.
13. Baker, H.E., Kiel, A.M., Luebbe, S.T., Simon, B.R., Earl, C.C., Regmi, A., Roell, W.C., Mather, K.J., Tune, J.D., and Goodwill, A.G. (2019). Inhibition of sodium-glucose cotransporter-2 preserves cardiac function during regional myocardial ischemia independent of alterations in myocardial substrate utilization. Basic research in cardiology *114*, 25. 10.1007/s00395-019-0733-2.
14. He, L., Ma, S., Zuo, Q., Zhang, G., Wang, Z., Zhang, T., Zhai, J., and Guo, Y. (2022). An Effective Sodium-Dependent Glucose Transporter 2 Inhibition, Canagliflozin, Prevents Development of Hypertensive Heart Failure in Dahl Salt-Sensitive Rats. Frontiers in pharmacology *13*, 856386. 10.3389/fphar.2022.856386.
15. Konopka, A.R., and Harber, M.P. (2014). Skeletal muscle hypertrophy after aerobic exercise training. Exercise and sport sciences reviews *42*, 53-61. 10.1249/jes.0000000000000007.
16. Gomes, M.J., Pagan, L.U., Lima, A.R.R., Reyes, D.R.A., Martinez, P.F., Damatto, F.C., Pontes, T.H.D., Rodrigues, E.A., Souza, L.M., Tosta, I.F., et al. (2020). Effects of aerobic and resistance exercise on cardiac remodelling and skeletal muscle oxidative stress of infarcted rats. Journal of cellular and molecular medicine *24*, 5352-5362. 10.1111/jcmm.15191.
17. Bozkurt, B., Fonarow, G.C., Goldberg, L.R., Guglin, M., Josephson, R.A., Forman, D.E., Lin, G., Lindenfeld, J., O'Connor, C., Panjrath, G., et al. (2021). Cardiac Rehabilitation for Patients With Heart Failure: JACC Expert Panel. Journal of the American College of Cardiology *77*, 1454-1469. 10.1016/j.jacc.2021.01.030.
18. Stølen, T., Shi, M., Wohlwend, M., Høydal, M.A., Bathen, T.F., Ellingsen, Ø., and Esmaeili, M. (2020). Effect of exercise training on cardiac metabolism in rats with heart failure. Scandinavian cardiovascular journal : SCJ *54*, 84-91. 10.1080/14017431.2019.1658893.
19. Xie, C., Zhang, Y., Tran, T.D., Wang, H., Li, S., George, E.V., Zhuang, H., Zhang, P., Kandel, A., Lai, Y., et al. (2015). Irisin Controls Growth, Intracellular Ca2+ Signals, and Mitochondrial Thermogenesis in Cardiomyoblasts. PloS one *10*, e0136816. 10.1371/journal.pone.0136816.
20. Keihanian, F., Moohebati, M., Saeidinia, A., Mohajeri, S.A., and Madaeni, S. (2021). Therapeutic effects of medicinal plants on isoproterenol-induced heart failure in rats. Biomedicine & pharmacotherapy = Biomedecine & pharmacotherapie *134*, 111101. 10.1016/j.biopha.2020.111101.

21. Liu, M., Ai, J., Feng, J., Zheng, J., Tang, K., Shuai, Z., and Yang, J. (2019). Effect of paeoniflorin on cardiac remodeling in chronic heart failure rats through the transforming growth factor β1/Smad signaling pathway. Cardiovasc Diagn Ther *9*, 272-280. 10.21037/cdt.2019.06.01.
22. Hira, T., Koga, T., Sasaki, K., and Hara, H. (2017). Canagliflozin potentiates GLP-1 secretion and lowers the peak of GIP secretion in rats fed a high-fat high-sucrose diet. Biochemical and biophysical research communications *492*, 161-165. 10.1016/j.bbrc.2017.08.031.
23. Bedford, T.G., Tipton, C.M., Wilson, N.C., Oppliger, R.A., and Gisolfi, C.V. (1979). Maximum oxygen consumption of rats and its changes with various experimental procedures. Journal of applied physiology: respiratory, environmental and exercise physiology *47*, 1278-1283. 10.1152/jappl.1979.47.6.1278.
24. Szklarczyk, D., Gable, A.L., Nastou, K.C., Lyon, D., Kirsch, R., Pyysalo, S., Doncheva, N.T., Legeay, M., Fang, T., Bork, P., et al. (2021). The STRING database in 2021: customizable protein-protein networks, and functional characterization of user-uploaded gene/measurement sets. Nucleic acids research *49*, D605-d612. 10.1093/nar/gkaa1074.
25. Bader, G.D., and Hogue, C.W. (2003). An automated method for finding molecular complexes in large protein interaction networks. BMC bioinformatics *4*, 2. 10.1186/1471-2105-4-2.
26. Shannon, P., Markiel, A., Ozier, O., Baliga, N.S., Wang, J.T., Ramage, D., Amin, N., Schwikowski, B., and Ideker, T. (2003). Cytoscape: a software environment for integrated models of biomolecular interaction networks. Genome Res *13*, 2498-2504. 10.1101/gr.1239303.
27. Zhou, Y., Zhou, B., Pache, L., Chang, M., Khodabakhshi, A.H., Tanaseichuk, O., Benner, C., and Chanda, S.K. (2019). Metascape provides a biologist-oriented resource for the analysis of systems-level datasets. Nature communications *10*, 1523. 10.1038/s41467-019-09234-6.
28. Wang, L., Tian, X., Cao, Y., Ma, X., Shang, L., Li, H., Zhang, X., Deng, F., Li, S., Guo, T., and Yang, P. (2021). Cardiac Shock Wave Therapy Improves Ventricular Function by Relieving Fibrosis Through PI3K/Akt Signaling Pathway: Evidence From a Rat Model of Post-infarction Heart Failure. Frontiers in cardiovascular medicine *8*, 693875. 10.3389/fcvm.2021.693875.
29. Li, L., Fang, H., Yu, Y.H., Liu, S.X., and Yang, Z.Q. (2021). Liquiritigenin attenuates isoprenaline-induced myocardial fibrosis in mice through the TGF-β1/Smad2 and AKT/ERK signaling pathways. Molecular medicine reports *24*. 10.3892/mmr.2021.12326.
30. Gallo, S., Vitacolonna, A., Bonzano, A., Comoglio, P., and Crepaldi, T. (2019). ERK: A Key Player in the Pathophysiology of Cardiac Hypertrophy. International journal of molecular sciences *20*. 10.3390/ijms20092164.
31. Sussman, M.A., Völkers, M., Fischer, K., Bailey, B., Cottage, C.T., Din, S., Gude, N., Avitabile, D., Alvarez, R., Sundararaman, B., et al. (2011). Myocardial AKT: the omnipresent nexus. Physiological reviews *91*, 1023-1070. 10.1152/physrev.00024.2010.
32. Lu, M., Qin, Q., Yao, J., Sun, L., and Qin, X. (2019). Induction of LOX by TGF-β1/Smad/AP-1 signaling aggravates rat myocardial fibrosis and heart failure. IUBMB life *71*, 1729-1739. 10.1002/iub.2112.
33. Lopaschuk, G.D., Karwi, Q.G., Tian, R., Wende, A.R., and Abel, E.D. (2021). Cardiac Energy Metabolism in Heart Failure. Circulation research *128*, 1487-1513. 10.1161/circresaha.121.318241.
34. Chen, C.H., Ke, L.Y., Chan, H.C., Lee, A.S., Lin, K.D., Chu, C.S., Lee, M.Y., Hsiao, P.J., Hsu, C., Chen, C.H., and Shin, S.J. (2016). Electronegative low density lipoprotein induces renal apoptosis and fibrosis: STRA6 signaling involved. Journal of lipid research *57*, 1435-1446. 10.1194/jlr.M067215.
35. Ono, K., Sandell, L.L., Trainor, P.A., and Wu, D.K. (2020). Retinoic acid synthesis and autoregulation mediate zonal patterning of vestibular organs and inner ear morphogenesis. Development (Cambridge, England) *147*. 10.1242/dev.192070.
36. Choudhary, R., Palm-Leis, A., Scott, R.C., 3rd, Guleria, R.S., Rachut, E., Baker, K.M., and Pan, J. (2008). All-trans retinoic acid prevents development of cardiac remodeling in aortic banded rats by inhibiting the renin-angiotensin system. American journal of physiology. Heart and circulatory physiology *294*, H633-644. 10.1152/ajpheart.01301.2007.
37. Pavan, M., Ruiz, V.F., Silva, F.A., Sobreira, T.J., Cravo, R.M., Vasconcelos, M., Marques, L.P., Mesquita, S.M., Krieger, J.E., Lopes, A.A., et al. (2009). ALDH1A2 (RALDH2) genetic variation in human congenital heart disease. BMC medical genetics *10*, 113. 10.1186/1471-2350-10-113.
38. Steiner, M.B., Vengoechea, J., and Collins, R.T., 2nd (2013). Duplication of the ALDH1A2 gene in association with pentalogy of Cantrell: a case report. Journal of medical case reports *7*, 287. 10.1186/1752-1947-7-287.
39. Sandell, L.L., Sanderson, B.W., Moiseyev, G., Johnson, T., Mushegian, A., Young, K., Rey, J.P., Ma, J.X., Staehling-Hampton, K., and Trainor, P.A. (2007). RDH10 is essential for synthesis of embryonic retinoic acid and is required for limb, craniofacial, and organ development. Genes & development *21*, 1113-1124. 10.1101/gad.1533407.

40. Roman, R.J. (2002). P-450 metabolites of arachidonic acid in the control of cardiovascular function. Physiological reviews *82*, 131-185. 10.1152/physrev.00021.2001.
41. Althurwi, H.N., Elshenawy, O.H., and El-Kadi, A.O. (2014). Fenofibrate modulates cytochrome P450 and arachidonic acid metabolism in the heart and protects against isoproterenol-induced cardiac hypertrophy. Journal of cardiovascular pharmacology *63*, 167-177. 10.1097/fjc.0000000000000036.
42. Jiang, S., Huo, D., Wang, X., Zhao, H., Tan, J., Zeng, Q., O'Rourke, S.T., and Sun, C. (2017). β-adrenergic Receptor-stimulated Cardiac Myocyte Apoptosis: Role of Cytochrome P450 ω-hydroxylase. Journal of cardiovascular pharmacology *70*, 94-101. 10.1097/fjc.0000000000000499.
43. Zeng, Z., Wang, Q., Yang, X., Ren, Y., Jiao, S., Zhu, Q., Guo, D., Xia, K., Wang, Y., Li, C., and Wang, W. (2019). Qishen granule attenuates cardiac fibrosis by regulating TGF-β /Smad3 and GSK-3β pathway. Phytomedicine *62*, 152949. 10.1016/j.phymed.2019.152949.
44. Badolia, R., Manne, B.K., Dangelmaier, C., Chernoff, J., and Kunapuli, S.P. (2015). Gq-mediated Akt translocation to the membrane: a novel PIP3-independent mechanism in platelets. Blood *125*, 175-184. 10.1182/blood-2014-05-576306.
45. Ruppert, C., Deiss, K., Herrmann, S., Vidal, M., Oezkur, M., Gorski, A., Weidemann, F., Lohse, M.J., and Lorenz, K. (2013). Interference with ERK(Thr188) phosphorylation impairs pathological but not physiological cardiac hypertrophy. Proc Natl Acad Sci U S A *110*, 7440-7445. 10.1073/pnas.1221999110.
46. Redondo, S., Santos-Gallego, C.G., and Tejerina, T. (2007). TGF-beta1: a novel target for cardiovascular pharmacology. Cytokine Growth Factor Rev *18*, 279-286. 10.1016/j.cytogfr.2007.04.005.
47. Lee, K.S., Park, S.J., Kim, S.R., Min, K.H., Lee, K.Y., Choe, Y.H., Hong, S.H., Lee, Y.R., Kim, J.S., Hong, S.J., and Lee, Y.C. (2008). Inhibition of VEGF blocks TGF-beta1 production through a PI3K/Akt signalling pathway. Eur Respir J *31*, 523-531. 10.1183/09031936.00125007.
48. Tang, Q., Markby, G.R., MacNair, A.J., Tang, K., Tkacz, M., Parys, M., Phadwal, K., MacRae, V.E., and Corcoran, B.M. (2023). TGF-β-induced PI3K/AKT/mTOR pathway controls myofibroblast differentiation and secretory phenotype of valvular interstitial cells through the modulation of cellular senescence in a naturally occurring in vitro canine model of myxomatous mitral valve disease. Cell Prolif *56*, e13435. 10.1111/cpr.13435.
49. Wei, W.Y., Ma, Z.G., Xu, S.C., Zhang, N., and Tang, Q.Z. (2016). Pioglitazone Protected against Cardiac Hypertrophy via Inhibiting AKT/GSK3β and MAPK Signaling Pathways. PPAR research *2016*, 9174190. 10.1155/2016/9174190.
50. Gao, G., Jiang, S., Ge, L., Zhang, S., Zhai, C., Chen, W., and Sui, S. (2019). Atorvastatin Improves Doxorubicin-Induced Cardiac Dysfunction by Modulating Hsp70, Akt, and MAPK Signaling Pathways. Journal of cardiovascular pharmacology *73*, 223-231. 10.1097/fjc.0000000000000646.
51. Tao, H., Xu, W., Qu, W., Gao, H., Zhang, J., Cheng, X., Liu, N., Chen, J., Xu, G.L., Li, X., and Shu, Q. (2021). Loss of ten-eleven translocation 2 induces cardiac hypertrophy and fibrosis through modulating ERK signaling pathway. Human molecular genetics *30*, 865-879. 10.1093/hmg/ddab046.

TABLE 1. Canagliflozin combined with aerobic exercise improved left ventricular function in ISO-induced rats.

Group	Control	ISO	ISO+AE	ISO+CA	ISO+CA+AE
LVPWd (mm)	2.64±0.47	2.33±0.12	2.42±0.26	2.28±0.16	2.46±0.17
LVPWs (mm)	3.31±0.35	3.35±0.26	3.56±0.35	3.76±0.17	3.92±0.23
LVAWd (mm)	2.74±0.22	2.05±0.21	2.23±0.13	2.17±0.15	2.49±0.20
LVAWs (mm)	4.04±0.06	2.71±0.20$^{\#\#}$	3.14±0.24	2.99±0.10	3.21±0.32
LVIDd (mm)	7.11±0.31	6.73±0.04	6.09±0.30	7.01±0.39	6.64±0.61
LVIDs (mm)	2.86±0.38	4.16±0.28$^{\#\#}$	2.67±0.25***	3.56±0.26	3.39±0.32*
LVEDV (ul)	272.20±29.05	248.80±7.02	159.40±18.84***	260.10±32.15	237.00±54.53
LVESV (ul)	60.15±11.05	111.40±18.51$^{\#\#}$	43.03±8.68***	74.01±10.62	56.47±13.57**

ISO: isoproterenol-treated group; ISO + AE: ISO + aerobic exercise group. ISO + CA: ISO + canagliflozin. ISO + AE + CA: ISO + aerobic exercise + canagliflozin. LVPWd: left ventricular posterior wall thickness at end-diastole. LVPWs: left ventricular posterior wall thickness at end systole. LVAWd: left ventricular anterior wall diastole. LVAWs: left ventricular end systolic anterior wall thickness. LVIDd: left ventricular end-diastolic inner-dimension. LVIDs: left ventricular end-systolic inner-dimension. LVEDV: left ventricular end-diastolic volume. LVESV: left ventricular end-systolic volume. The results are expressed as mean ± SEM of n = 5 per group. Significance: # $P < 0.05$ vs. control group; ## $P < 0.01$ vs. control group; #### $P < 0.0001$ vs. control group; * $P < 0.05$ vs. ISO group; **P <0.01 vs. ISO group; *** $P < 0.001$ vs. lSO group. Data are represented as mean ±SEM.

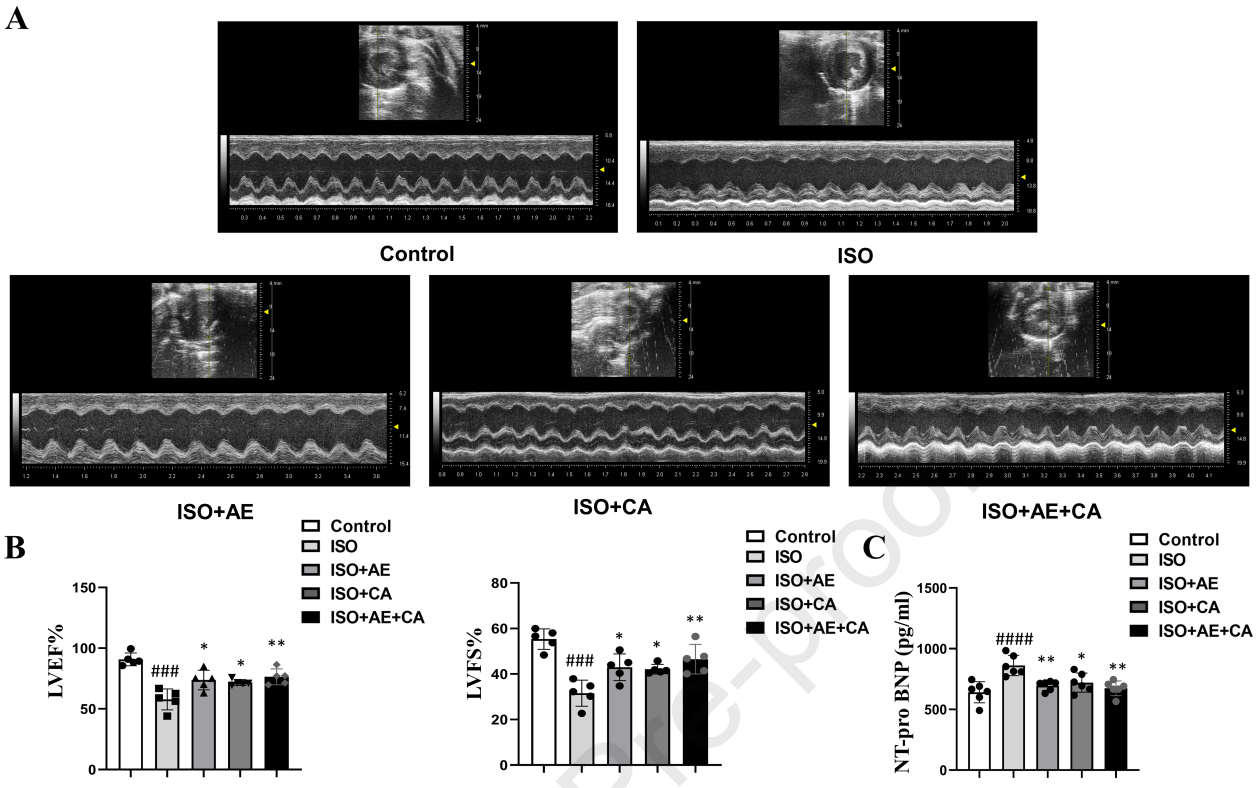

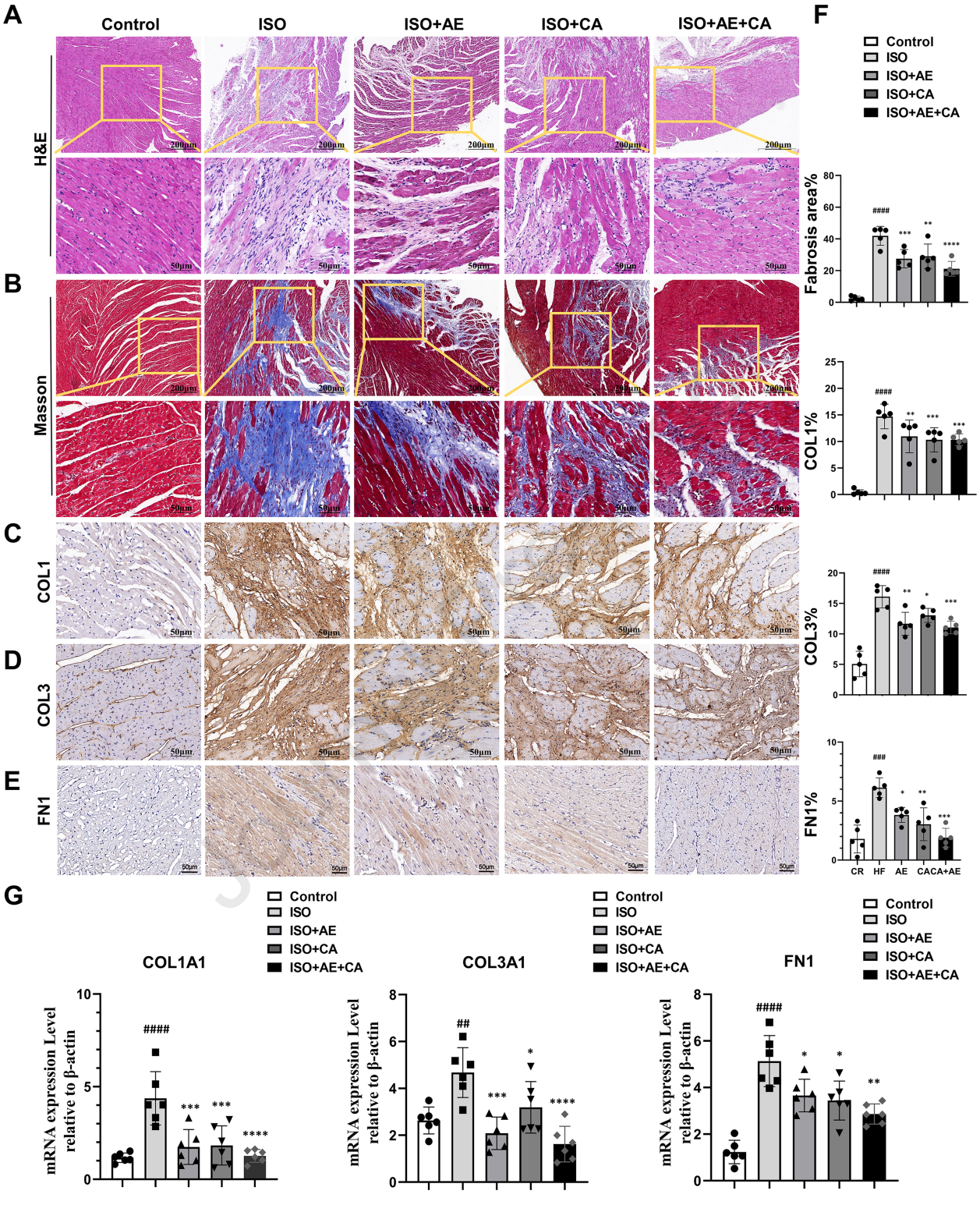
A
Control
ISO
ISO+AE
ISO+CA
ISO+AE+CA
H&E
B
Masson
C
COL1
D
COL3
E
FN1
F
Control
ISO
ISO+AE
ISO+CA
ISO+AE+CA
Fabrosis area%
COL1%
COL3%
FN1%
CR
HF
AE
CACA+AE
G
COL1A1
COL3A1
FN1
mRNA expression Level relative to β-actin

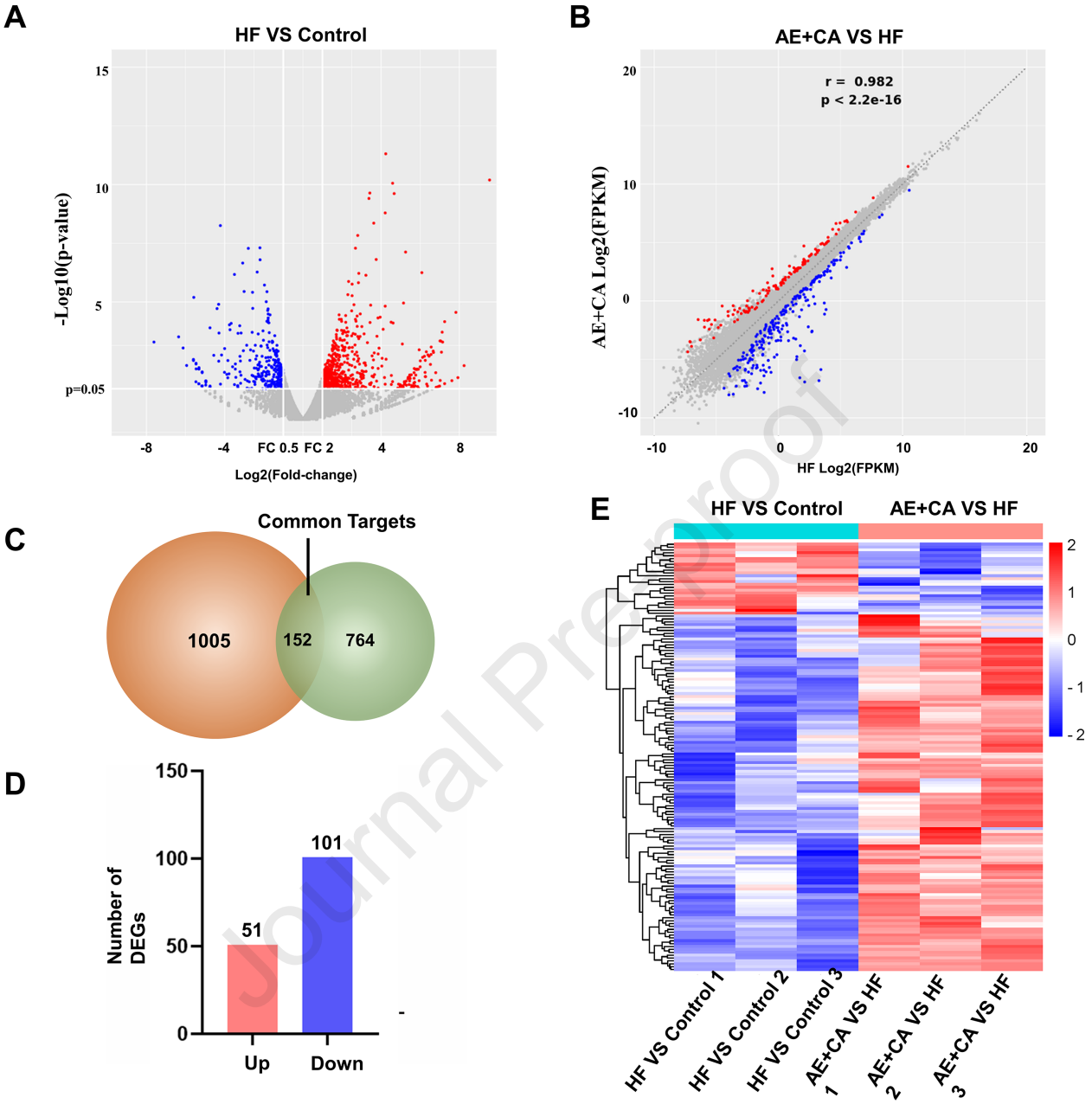

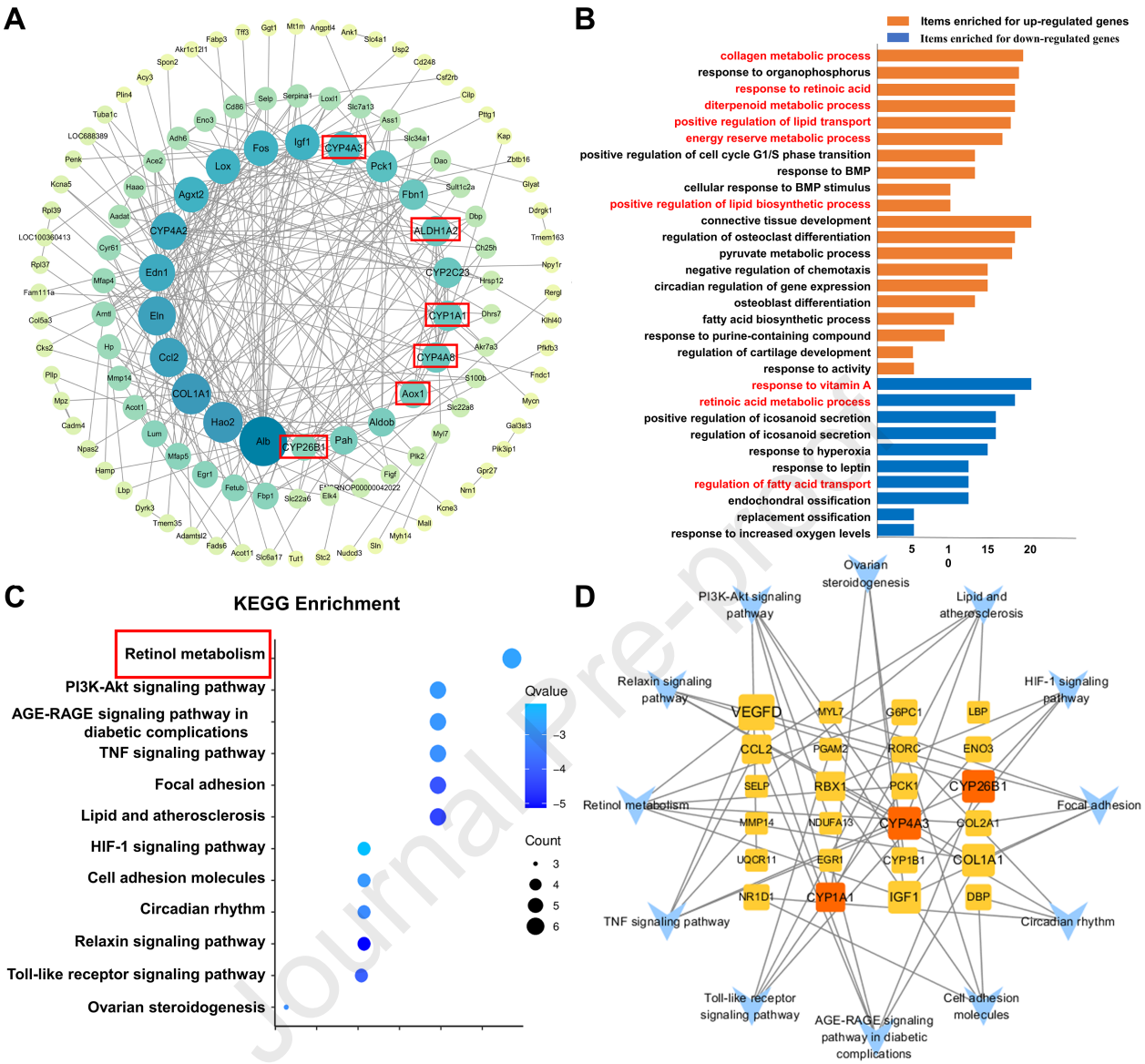

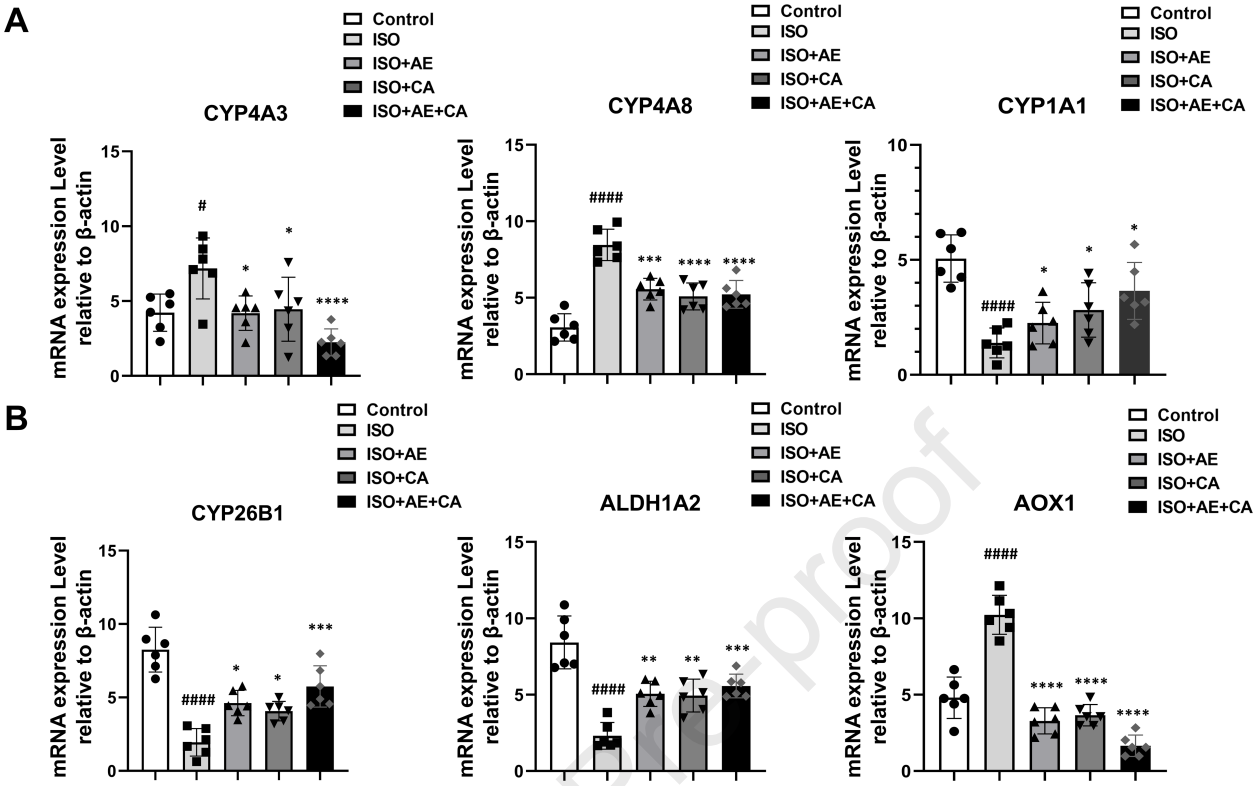

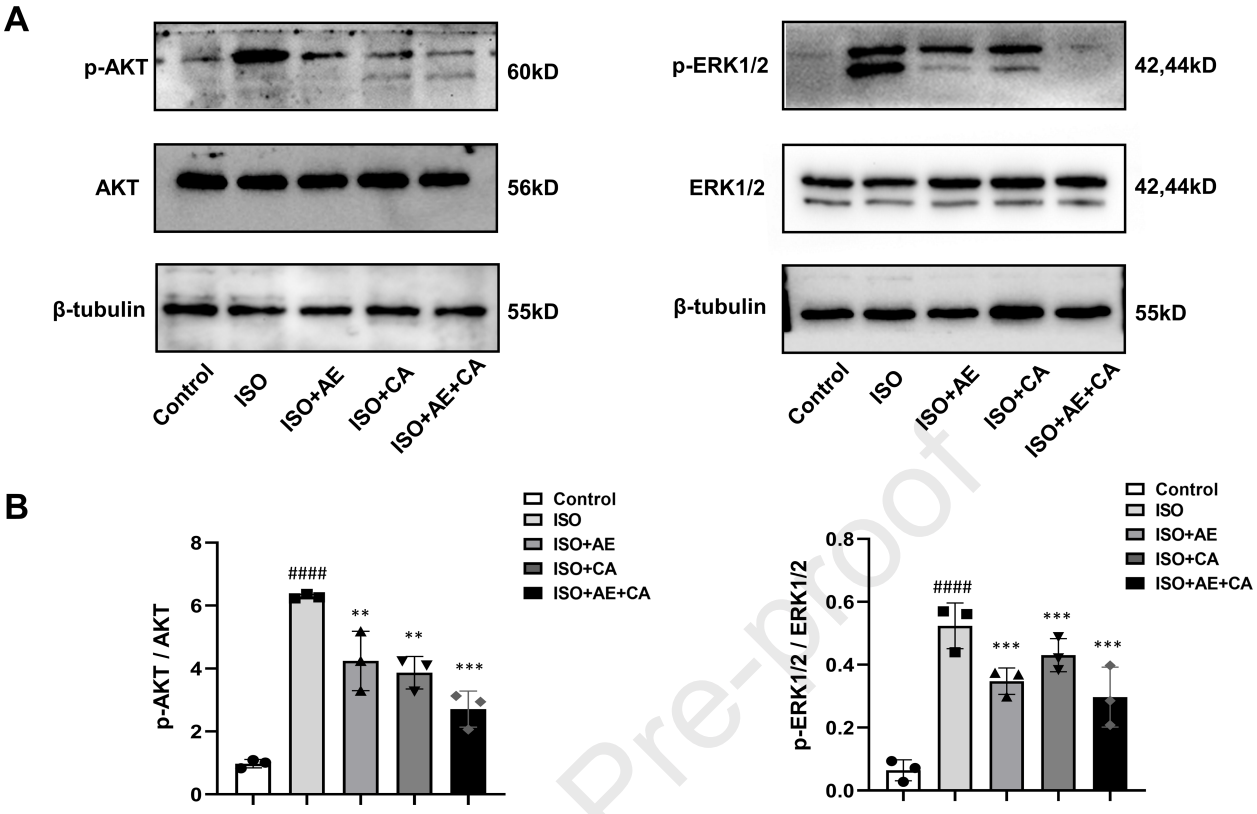

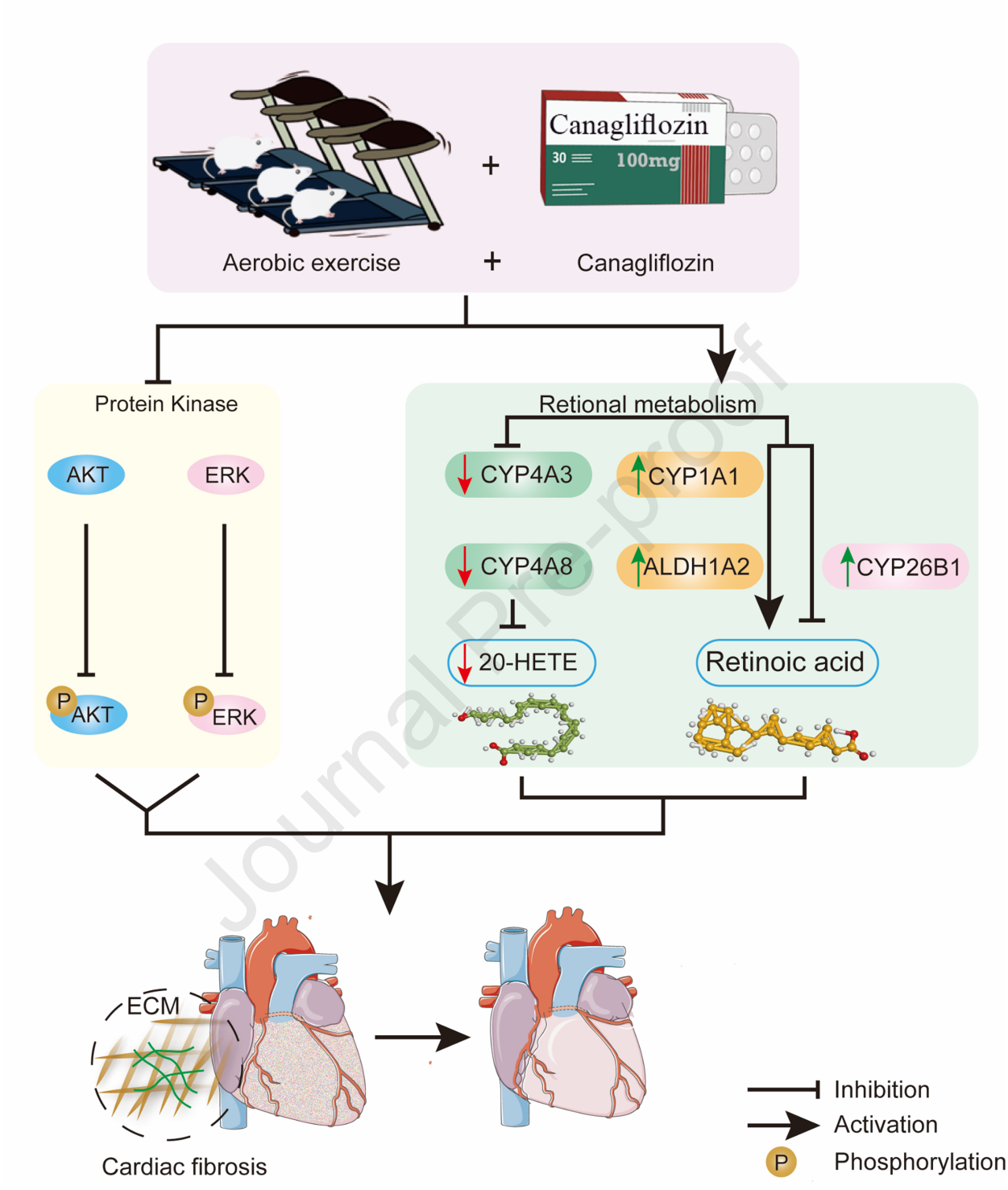

Please format the Highlights as per our guide to the authors. Highlights are bullet points that convey the core findings of your paper. You may include up to four highlights. The length of each highlight cannot exceed 85 characters (including spaces). On the EM page where you are asked to upload your files, please choose "Highlights" and upload as a Word document.

(1) Canagliflozin combined with aerobic exercise improve chronic heart failure.

(2) Canagliflozin combined with aerobic exercise reduces myocardial fibrosis.

(3) Canagliflozin combined with aerobic exercise inhibits the AKT/ERK signaling pathway.

(4) The retinol metabolism signaling pathway plays a role in chronic heart failure.

CellPress

KEY RESOURCES TABLE

The table highlights the reagents, genetically modified organisms and strains, cell lines, software, instrumentation, and source data **essential** to reproduce results presented in the manuscript. Depending on the nature of the study, this may include standard laboratory materials (i.e., food chow for metabolism studies, support material for catalysis studies), but the table is **not** meant to be a comprehensive list of all materials and resources used (e.g., essential chemicals such as standard solvents, SDS, sucrose, or standard culture media do not need to be listed in the table). **However, please note that items in the table must also be reported in the method details section within the context of their use.**

ALL references cited in the key resources table must be included in the main references list. Citations should be formatted as "Author name et al.[#]" (e.g., Smith et al.[1]), with the citation number matching that in the main references list.

Please report the information as follows:

- **REAGENT or RESOURCE:** Provide the full descriptive name of the item so that it can be identified and linked with its description in the manuscript (e.g., provide version number for software, host source for antibody, strain name). See the sample tables at the end of this document for examples of how to report reagents.
    - In the **experimental models sections** (applicable only to experimental life science studies), please include all models used in the paper and describe each line/strain as model organism: name used for strain/line in paper: genotype (e.g., Mouse: $OXTR^{fl/fl}$: B6.129(SJL)-$Oxtr^{tm1.1Wsy/J}$).
    - The **Biological samples section** (applicable only to experimental life science studies) should list all samples obtained in this study or from commercial sources or biological repositories.
    - **You may list a maximum of 10 oligonucleotides or RNA sequences** in the table. If there are more than 10 to report, please provide this information as a supplemental document and reference the file (e.g., See Table S1 for XX) in the key resources table.
    - **Deposited data** should include both newly deposited data from this manuscript and existing datasets that were used in the manuscript.
    - Please include software and code mentioned in the method details or data and code availability section under **software and algorithms**.
    - Any item that does not fit the existing subheadings should be added to the "other" section. **Please do not add your own subheadings.**
- **SOURCE:** Report the company, manufacturer, or individual that provided the item or where the item can be obtained (e.g., stock center or repository).
    - For materials distributed by Addgene, please cite the article describing the plasmid and include "Addgene" as part of the identifier.
    - If an item is from another lab, please include the name of the principal investigator and a citation if it has been previously published.
    - If the material is being reported for the first time in the current paper, please indicate as "this paper."
    - For software, please provide the company name if it is commercially available or cite the paper in which it has been initially described.
- **IDENTIFIER:** Include catalog numbers (entered in the column as "Cat#" followed by the number, e.g., Cat#3879S). Where available, please include unique entities such as RRIDs, Model Organism Database numbers, and accession numbers preceded by database abbreviations such as PDB or

CCDC). Please ensure the accuracy of the identifiers, as they are essential for generation of hyperlinks to external sources when available. For more information about data sharing policies and a list of recommended data repositories for abbreviations, please see the Cell Press Author's guide to data sharing.

- For antibodies, if applicable and available, please also include the lot number or clone identity.
- For software or data resources, please include the URL where the resource can be downloaded.
- When listing more than one identifier for the same item, use semicolons to separate them (e.g., Cat#3879S; RRID: AB_2255011).
- If an identifier is not available, please enter "N/A" in the column.
- ***A NOTE ABOUT RRIDs:*** we highly recommend using RRIDs as the identifier (in particular for antibodies and organisms but also for software tools and databases). For more details on how to obtain or generate an RRID for existing or newly generated resources, please visit the RII or search for RRIDs.

Please use the empty table that follows to organize the information under the provided subheadings and skip sections that are not relevant to your study. To add a row, place the cursor at the end of the row above where you would like to add the row, just outside the right border of the table. Then press the ENTER key to add the row. Alternatively, you can right-click on your mouse and choose Insert > Insert rows above or Insert rows below. Please delete empty rows. Each entry must be on a separate row; do not list multiple items in a single table cell. Please see the sample tables at the end of this document for relevant examples in the life and physical sciences of how reagents and instrumentation should be cited.

CellPress

TABLE FOR AUTHOR TO COMPLETE

Please do not add custom subheadings. *If you wish to make an entry that does not fall into one of the subheadings below, please contact your handling editor or add it under the "other"* subheading. ***Any subheadings not relevant to your study can be skipped.*** *(**NOTE:** references should be in numbered style, e.g., Smith et al.[1])*

Key resources table

REAGENT or RESOURCE	SOURCE	IDENTIFIER
Antibodies		
β -tubulin	Proteintech	10068-1-AP
AKT	Abcam	cat. no. ab32505
phosphorylated AKT	Abcam	cat. no. ab192623
ERK1/2	Abcam	cat. no. ab184699
phosphorylated ERK1/2	Abcam	cat. no. ab201015;
Bacterial and virus strains		
Biological samples		
heart tissue (rat)	This paper	N/A
Chemicals, peptides, and recombinant proteins		
Critical commercial assays		
Deposited data		
Experimental models: Cell lines		

Experimental models: Organisms/strains		
Mouse: Male Sprague Dawley (SD)	Beijing Weitong 99 Lihua Laboratory Animal Technology Co., Ltd.	002
Oligonucleotides		
R-COL1A1-S		CCCAGCGGTGGTTATGACTT
R-COL1A1-A		TCGATCCAGTACTCTCCGCT
R-COL3A1-S		CGAGGTAACAGAGGTGAAAGAGG
R-COL3A1-A		TTTCACCTCCAACTCCAGCAAT
R-FN1-S		AAACCTCTACGGGTCGCTG
R-FNI-A		GCGCTGGTGGTGAAGTCAAA
R-CYP1A1-S		GACATTTGAGAAGGGCCACATC
R-CYP1A1-A		GGTTGGTTACCAGGTACATGAGG
R-CYP2C23-S		AGAACTTGGCTGTCTGTGGGTC
R-CYP2C23-A		TCGGTATAAGGCAGCTTCATCT
R-ALDH1A2-S		TGGACGCTTCTGAAAGAGGAC
R-ALDH1A2-A		GGCTTACCGCCATTTAGTGATT
R-CYP4A8-S		CAGCACCGACGAATGTTGACT
R-CYP4A8-A		AACTGGACACTGCCCTCTTGG
R-CYP4A3-S		TGCTCAGTCTATTTCTGGTGCTG
R-CYP4A3-A		CCACGTAAGAACCTGCTGGAAT
R-CYP26B1-S		AGAGCTGCAAGCTGCCTATCC
R-CYP26B1-A		CTGGTGTTCGCCCAGTAGGAT
RB-ACTINS		TGCTATGTTGCCCTAGACTTCG

RB-ACTIN-A		GTTGGCATAGAGG TCTTTACGG
Recombinant DNA		
Software and algorithms		
ImageJ	National Institutes of Health	https://imagej.nih.gov/ij/
Cytoscape	Bloomage Biotechnol Corporation	3.7.1
GraphPad Prism 8	GraphPad	N/A
Other		

CellPress

SAMPLE TABLES FOR AUTHOR REFERENCE

LIFE SCIENCES

REAGENT or RESOURCE	SOURCE	IDENTIFIER
Antibodies		
Rabbit monoclonal anti-Snail	Cell Signaling Technology	Cat#3879S; RRID: AB_2255011
Mouse monoclonal anti-Tubulin (clone DM1A)	Sigma-Aldrich	Cat#T9026; RRID: AB_477593
Rabbit polyclonal anti-BMAL1	This paper	N/A
Bacterial and virus strains		
pAAV-hSyn-DIO-hM3D(Gq)-mCherry	Krashes et al.[1]	Addgene AAV5; 44361-AAV5
AAV5-EF1a-DIO-hChR2(H134R)-EYFP	Hope Center Viral Vectors Core	N/A
Cowpox virus Brighton Red	BEI Resources	NR-88
Zika-SMGC-1, GENBANK: KX266255	Isolated from patient (Wang et al.[2])	N/A
Staphylococcus aureus	ATCC	ATCC 29213
Streptococcus pyogenes: M1 serotype strain: strain SF370; M1 GAS	ATCC	ATCC 700294
Biological samples		
Healthy adult BA9 brain tissue	University of Maryland Brain & Tissue Bank; http://medschool.umaryland.edu/btbank/	Cat#UMB1455
Human hippocampal brain blocks	New York Brain Bank	http://nybb.hs.columbia.edu/
Patient-derived xenografts (PDX)	Children's Oncology Group Cell Culture and Xenograft Repository	http://cogcell.org/
Chemicals, peptides, and recombinant proteins		
MK-2206 AKT inhibitor	Selleck Chemicals	S1078; CAS: 1032350-13-2
SB-505124	Sigma-Aldrich	S4696; CAS: 694433-59-5 (free base)
Picrotoxin	Sigma-Aldrich	P1675; CAS: 124-87-8
Human TGF-β	R&D	240-B; GenPept: P01137
Activated S6K1	Millipore	Cat#14-486
GST-BMAL1	Novus	Cat#H00000406-P01
Critical commercial assays		
EasyTag EXPRESS 35S Protein Labeling Kit	PerkinElmer	NEG772014MC
CaspaseGlo 3/7	Promega	G8090
TruSeq ChIP Sample Prep Kit	Illumina	IP-202-1012
Deposited data		

Raw and analyzed data	This paper	GEO: GSE63473
B-RAF RBD (apo) structure	This paper	PDB: 5J17
Human reference genome NCBI build 37, GRCh37	Genome Reference Consortium	http://www.ncbi.nlm.nih.gov/projects/genome/assembly/grc/human/
Nanog STILT inference	This paper; Mendeley Data	http://dx.doi.org/10.17632/wx6s4mj7s8.2
Affinity-based mass spectrometry performed with 57 genes	This paper; Mendeley Data	Table S8; http://dx.doi.org/10.17632/5hvpvspw82.1
Experimental models: Cell lines		
Hamster: CHO cells	ATCC	CRL-11268
D. melanogaster: Cell line S2: S2-DRSC	Laboratory of Norbert Perrimon	FlyBase: FBtc0000181
Human: Passage 40 H9 ES cells	MSKCC stem cell core facility	N/A
Human: HUES 8 hESC line (NIH approval number NIHhESC-09-0021)	HSCI iPS Core	hES Cell Line: HUES-8
Experimental models: Organisms/strains		
C. elegans: Strain BC4011: srl-1(s2500) II; dpy-18(e364) III; unc-46(e177)rol-3(s1040) V.	Caenorhabditis Genetics Center	WB Strain: BC4011; WormBase: WBVar00241916
D. melanogaster: RNAi of Sxl: y[1] sc[*] v[1]; P{TRiP.HMS00609}attP2	Bloomington Drosophila Stock Center	BDSC:34393; FlyBase: FBtp0064874
S. cerevisiae: Strain background: W303	ATCC	ATTC: 208353
Mouse: R6/2: B6CBA-Tg(HDexon1)62Gpb/3J	The Jackson Laboratory	JAX: 006494
Mouse: OXTRfl/fl: B6.129(SJL)-Oxtr$^{tm1.1Wsy}$/J	The Jackson Laboratory	RRID: IMSR_JAX:008471
Zebrafish: Tg(Shha:GFP)t10: t10Tg	Neumann and Nuesslein-Volhard[3]	ZFIN: ZDB-GENO-060207-1
Arabidopsis: 35S::PIF4-YFP, BZR1-CFP	Wang et al.[4]	N/A
Arabidopsis: JYB1021.2: pS24(AT5G58010)::cS24:GFP(-G):NOS #1	NASC	NASC ID: N70450
Oligonucleotides		
siRNA targeting sequence: PIP5K I alpha #1: ACACAGUACUCAGUUGAUA	This paper	N/A
Primers for XX, see Table SX	This paper	N/A
Primer: GFP/YFP/CFP Forward: GCACGACTTCTTCAAGTCCGCCATGCC	This paper	N/A
Morpholino: MO-pax2a GGTCTGCTTTGCAGTGAATATCCAT	Gene Tools	ZFIN: ZDB-MRPHLNO-061106-5
ACTB (hs01060665_g1)	Life Technologies	Cat#4331182
RNA sequence: hnRNPA1_ligand: UAGGGACUUAGGGUUCUCUCUAGGGACUUAGGGUUCUCUCUAGGGA	This paper	N/A
Recombinant DNA		

pLVX-Tight-Puro (TetOn)	Clonetech	Cat#632162
Plasmid: GFP-Nito	This paper	N/A
cDNA GH111110	Drosophila Genomics Resource Center	DGRC:5666; FlyBase:FBcl0130415
AAV2/1-hsyn-GCaMP6- WPRE	Chen et al.[5]	N/A
Mouse raptor: pLKO mouse shRNA 1 raptor	Thoreen et al.[6]	Addgene Plasmid #21339
Software and algorithms		
ImageJ	Schneider et al.[7]	https://imagej.nih.gov/ij/
Bowtie2	Langmead and Salzberg[8]	http://bowtie-bio.sourceforge.net/bowtie2/index.shtml
Samtools	Li et al.[9]	http://samtools.sourceforge.net/
Weighted Maximal Information Component Analysis v0.9	Rau et al.[10]	https://github.com/ChristophRau/wMICA
ICS algorithm	This paper; Mendeley Data	http://dx.doi.org/10.17632/5hvpvspw82.1
Other		
Sequence data, analyses, and resources related to the ultra-deep sequencing of the AML31 tumor, relapse, and matched normal	This paper	http://aml31.genome.wustl.edu
Resource website for the AML31 publication	This paper	https://github.com/chrisamiller/aml31SuppSite

PHYSICAL SCIENCES

REAGENT or RESOURCE	SOURCE	IDENTIFIER
Chemicals, peptides, and recombinant proteins		
QD605 streptavidin conjugated quantum dot	Thermo Fisher Scientific	Cat#Q10101MP
Platinum black	Sigma-Aldrich	Cat#205915
Sodium formate BioUltra, ≥99.0% (NT)	Sigma-Aldrich	Cat#71359
Chloramphenicol	Sigma-Aldrich	Cat#C0378
Carbon dioxide (^{13}C, 99%) (<2% ^{18}O)	Cambridge Isotope Laboratories	CLM-185-5
Poly(vinylidene fluoride-co-hexafluoropropylene)	Sigma-Aldrich	427179
PTFE Hydrophilic Membrane Filters, 0.22 μm, 90 mm	Scientificfilters.com/Tisch Scientific	SF13842
Critical commercial assays		
Folic Acid (FA) ELISA kit	Alpha Diagnostic International	Cat# 0365-0B9
TMT10plex Isobaric Label Reagent Set	Thermo Fisher	A37725
Surface Plasmon Resonance CM5 kit	GE Healthcare	Cat#29104988
NanoBRET Target Engagement K-5 kit	Promega	Cat#N2500
Deposited data		
B-RAF RBD (apo) structure	This paper	PDB: 5J17
Structure of compound 5	This paper; Cambridge Crystallographic Data Center	CCDC: 2016466
Code for constraints-based modeling and analysis of autotrophic *E. coli*	This paper	https://gitlab.com/elad.noor/sloppy/tree/master/rubisco
Software and algorithms		
Gaussian09	Frish et al.[1]	https://gaussian.com
Python version 2.7	Python Software Foundation	https://www.python.org
ChemDraw Professional 18.0	PerkinElmer	https://www.perkinelmer.com/category/chemdraw
Weighted Maximal Information Component Analysis v0.9	Rau et al.[2]	https://github.com/ChristophRau/wMICA
Other		
DASGIP MX4/4 Gas Mixing Module for 4 Vessels with a Mass Flow Controller	Eppendorf	Cat#76DGMX44
Agilent 1200 series HPLC	Agilent Technologies	https://www.agilent.com/en/products/liquid-chromatography
PHI Quantera II XPS	ULVAC-PHI, Inc.	https://www.ulvac-phi.com/en/products/xps/phi-quantera-ii/